12-2016

Antibacterial Activity and Chemical Characterization of Resin from *Sciadopitys verticillata* (Thunb.) Siebold and Zuccarini

David Ira Yates
University of Tennessee, Knoxville, dyates4@vols.utk.edu

To the Graduate Council:

I am submitting herewith a dissertation written by David Ira Yates entitled "Antibacterial Activity and Chemical Characterization of Resin from *Sciadopitys verticillata* (Thunb.) Siebold and Zuccarini." I have examined the final electronic copy of this dissertation for form and content and recommend that it be accepted in partial fulfillment of the requirements for the degree of Doctor of Philosophy, with a major in Plants, Soils, and Insects.

Kimberly D. Gwinn, Major Professor

We have read this dissertation and recommend its acceptance:

Bonnie H. Ownley, Earnest C. Bernard, William E. Klingeman III, Nicole Labbe

Accepted for the Council:

Carolyn R. Hodges

Vice Provost and Dean of the Graduate School

(Original signatures are on file with official student records.)

Antibacterial Activity and Chemical Characterization of Resin from *Sciadopitys verticillata* (Thunb.) Siebold and Zuccarini

A Dissertation Presented for the

Doctor of Philosophy

Degree

The University of Tennessee, Knoxville

David Ira Yates

December 2016

DEDICATION

To my father

Kelly Charles Yates

and my wife

Lisa Yates

ACKNOWLEDGEMENTS

I would like to express my deep gratitude to Mary Dee for her help and laboratory expertise during my graduate research. I would also like to thank Emma Batson for her help with statistical analysis of my data. I would like to especially thank my mentor, Dr. Kimberly D. Gwinn for her patience, advice, knowledge, hard work, prodding, and friendship throughout this difficult process.

ABSTRACT

Sciadopitys verticillata produces white viscous resin that is unique among the conifers. This research investigated effects of resin on bacteria from different ecological niches and the chemical composition of the resin. Each bacterial species was evaluated separately for response to winter- and summer-collected resins. Exposure to winter-collected resin reduced numbers of colonies of *Bacillus cereus*, *Erwinia amylovora*, *Agrobacterium tumefaciens*, and *Escherichia coli* and increased numbers of *Xanthomonas campestris*, *Pseudomonas fluorescens*, and *Pseudomonas syringae.* Summer-collected resin affected population growth of two bacterial species; population counts of *E. amylovora* decreased and those of *P. fluorescens* increased. Selected strains of *P. fluorescens* are active against *E. amylovora*.

Nuclear magnetic resonance (NMR), Fourier transform infrared spectroscopy (FTIR), gas chromatography mass spectrometry (GCMS), and pyrolysis GCMS were used to characterize chemical composition of resin of *S. verticillata*. Resin contained aldehydes, aromatics, olefins, alkoxy groups, ethers, alkyls, and carbonyls. Dimethyl sulfoxide extracts of resin containedα-pinene, tricyclene, and β-pinene (approximately 95% of total volatiles in GCMS analysis). In FTIR analysis, functional groups consistent with previous reports were identified. Analysis supported the proposals that *S. verticillata* resin is chemically similar to Cupressaceous resins but no Pineaecous resins.

Principal component analysis, coupled with pyrolysis GCMS spectrometry data, was used to screen for differences among *S. verticillata* trees grown in eastern Tennessee. Resin from four of six different source trees had no obvious differences. Differences in pyrograms of resins from two genetically identical trees that received different amounts of light were functional groups

normally associated with photosynthesis products; these products were low in abundance (1% or less) and low molecular weight. Principal component analysis was coupled with FTIR to evaluate differences between resin collected from *S. verticillata* and Frasier fir. Fraser fir was distinct from *S. verticillata* and did not contain the spectral signature of *S. verticillata* and other resins from plants believed to be related to *S. verticillata*.

This research is the most comprehensive study of resins collected from *S. verticillata* to date. *C*hemical basis of antimicrobial activity was not fully elucidated. Future research will address the role of chemical composition and resin concentration on antibacterial activity.

TABLE OF CONTENTS

Page

LIST OF TABLES

Page

LIST OF FIGURES

Page

LIST OF ABBREVIATIONS AND SYMBOLS

α	Alpha
β	Beta
mL	Milliliter
μL	Microliter
mg	Milligram
μg	Microgram
PCA	Principle Component Analysis
LN	Laurels Nursery tree
HC	Hugh Conlon tree
VA	Veterans Administration tree
WG	Wintergreen tree
UT	University of Tennessee tree
FL	Foster Levy tree

CHAPTER 1: Introduction

Background. Control of bacteria that cause plant disease, crop spoilage, food contamination, and infectious diseases of humans and animals is needed to provide a safe food supply (Khalil *et al*., 2009; Silva *et al*., 2010; García-Lomillo *et al*., 2014; Devcich *et al*., 2007). Use of antibiotics for control of plant disease is controversial, even though less than 1% of the antibiotics used in agriculture are employed to treat plant disease, and some antibiotics have been used for decades without reported adverse effects on humans or the environment (Stockwell *et al*., 2012,). Also, many of the current antimicrobials, such as penicillin, are generally ineffective and may cause an allergic reaction (Stockwell *et al*., 2012).

Plants produce bioactive compounds that are potential sources of new antimicrobials and platform compounds for the synthesis of new antibiotics (Cowan *et al*., 1999; Tiwari *et al*., 2009; Shults *et al*., 2014; Widsten *et al*., 2014; Cantrell *et al*., 2012). One limitation of plant-based materials for biopesticides is supply of raw materials, therefore renewable bioactive products that can be extracted from fruits, leaves, and resins of living perennial plants are especially attractive because they are renewable resources. Perennial plants produce a yearly supply of valuable extracts to producers, processors, and consumers. Plant resins are not only an established, viable, and renewable source of products, such as rubber and meat tenderizing enzymes, but resins are also potential sources of future novel antimicrobial agents for use in agricultural and food safety.

Resins of some plants have been studied extensively due to availability and economic value, while research on resins of less economically important and rare conifer species is limited. Conifer resins contain terpenoids, carboxylic acids and associated alcohols produced by secondary metabolism (Wolfe *et al*., 2009; Langenheim, 1994).All families and most genera of

conifers produce terpenoid resins (Langenheim, 1994). Conifer resins can be subdivided quantitatively into two types based on terpenoid constituents, and these broadly parallel conifer families: pinaceous resin (primarily abietane/pimarane diterpenes,) and cupressaceous resin (primarily labdanoid diterpenes). Some pinaceous resins are also volatile-rich resins (Tappert *et al*., 2011).

Terpenoids, produced by melvonic acid and deoxyxylulose phosphate pathways, constitute the most diverse group of plant natural products (25000 known compounds) that commonly function in plant biochemical defense, signaling, and defensive resinosis upon injury, primarily from insects (Wolfe *et al*., 2009; Croteau *et al*., 2000; Mcgarvey *et al*., 1995; Langenheim, 1994; Trapp *et al*., 2001).

Sciadopitys verticillata (Thunb.) Siebold and Zuccarini (Sciadopityaceae) is one of the lesser studied resin producing conifers. Commonly known as Japanese Umbrella Pine, *S. verticillata* is a needled evergreen tree endemic to the temperate middle cloud forests of central and western Japan (Sadowski *et al*., 2016;Eckenwalder, 2009) (Figure 1). Its common name (Umbrella) and species name (*verticillata*) both refer to the unique arrangement of the needle-like leaves that radiate from the growing tip of the branches, similar to the spokes of a wagon wheel or the spokes of an umbrella (Florin 1931; Farjon 2005; Eckenwalder, 2009; Dörken *et al*., 2011). While the common name of this plant also contains the word “Pine”, it is not a member of the Pineaceae (Pine) family but is the sole surviving member of the Sciadopityaceae family (Li *et al*. 2016; Yang *et al*., 2012; Crisp *et al*., 2011). Studies based on biochemical analysis, morphology, and chloroplast DNA consistently place the phylogenetic position of *S. verticillata* basal to modern conifers and more closely related to the Cephalotaxaceae, Taxaceae, and

Cupressaceae families than to the pines,(Sadowski *et al*., 2016; Li *et al*., 2016; Yang *et al*., 2012; Crisp *et al*., 2011). Russian researchers have rejected the use of the family name Sciadopityaceae and, based solely on leaf morphology, prefer the use of the family name Miroviaceae that includes the genera *Arctopitys*, *Holkopitys*, *Sciadopityoides*, *Mirovia*, and *Tritaenia* (Nosova*et al*., 2015).

Figure 1. *Sciadopitys verticillata* branch. The rubber-like leaves of *S. verticillata* form a whorl that radiates from the tip of the branch.

Sciadopitys verticillata was once widely distributed throughout Eurasia, with *S. verticillata* resin, pollen, and fossilized wood deposits being discovered in France (Sadowski *et al*., 2016). This tree is also considered to be one of the major contributors to the formation of the Baltic amber deposits (Sadowski *et al*., 2016). *Sciadopitys verticillata* has been used for construction in Japan for hundreds of years and is highly prized by plant enthusiasts for its dark green rubber-like foliage, and due to its rarity and expense, it is often unavailable in the landscape garden centers (Li *et al*., 2016). There are currently several grafted cultivars and selections advertised for purchase, but availability has been extremely low in recent years. *Sciadopitys verticillata* specimens available for research are also rare, with larger trees typically being located in protected arboretums or in private collections. Owners of *S. verticillata* are

generally reluctant to allow the large amount of plant material needed for resin extraction to be removed from their trees for fear of stress, disease, and/or reduced appearance.

Sciadopitys verticillata is unique among conifers in that it produces a sticky viscous white latex-like resin that serves a protective function to the tree by quickly sealing wounds, preventing bacterial and fungal entry into the plant's interior, and by trapping insects (Cowan *et al*., 1999; Choudhary *et al*., 2014; Yates *et al*., 2006; Phillips, 1990) (Figure 2). This sealing of wounds by the resin is problematic when asexually propagating *S. verticillata* by rooting of stem cuttings since the resin forms a barrier preventing cell contact with rooting hormones (Yates *et al*., 2006). The resin is a complex mixture of solids, liquids, and volatile gases that quickly hardens to a brittle wax-like substance when exposed to the atmosphere, where the volatiles can escape (Chapuisat *et al*., 2007).

Figure 2. *Sciadopitys* resin exuding from stem. Resin of *Sciadopitys* quickly solidifies when exposed to the atmosphere forming an effective protective physical barrier against pathogen attack.

Bioactivity and volatiles. Unprocessed resin inhibited bacterial growth when directly applied to a culture (Yates *et al*., 2006) (Figure 3). Although resin collected in summer did not inhibit growth of *Escherichia coli*, preliminary tests indicate that resin collected in winter inhibited cellular growth (Yates *et al*., 2006).In additional preliminary antimicrobial experiments, an agar overlay method was employed to determine if antimicrobial compounds in the resin were volatile. *Bacillus cereus* did not grow on the medium overlay directly above divots in the medium containing resin (a clear inhibition zone); however, there were no inhibition zones water only control (Yates and Gwinn, unpublished data; Figure A.1).

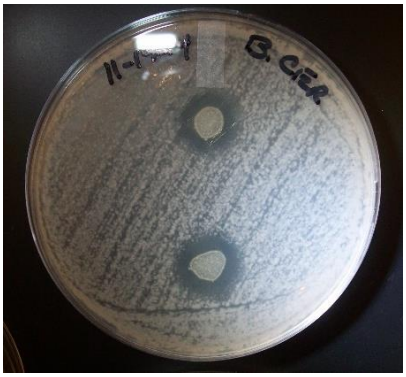

Figure 3. Inhibition zones in petri dish with *Bacillus* cereus – direct application method used in Yates *et al*., 2006.Clear inhibition zone are apparent around the resin application.

In order for the resin from *S. verticillata* resin or its bioactive components to be developed as a crop protection or food safety products, impact on bacteria that present threats to food safety, as well as those that affect plant health, must be determined, and the chemical basis of antibacterial activity must be elucidated. The objectives of this study were to: 1) identify

volatile compounds present in resin of *S. verticillata* and determine their antimicrobial activities; and 2) determine effect of season on activity of *S. verticillata* resin against key bacterial species. This study is the first known attempt to quantify the seasonal effect of resin from *S. verticillata* on bacteria and to use differences in seasonal resin chemistry detected by gas chromatography mass spectrometry (GC-MS) to identify the principal bioactive components responsible for the effect. This study is significant in that *S. verticillata* is a rare and understudied plant that may produce novel and/or beneficial products.

Little is known about the bioactivity and chemical composition of resin of *S. verticillata.* Bioactive compounds present in *S. verticillata* resin have reported antimicrobial effect when directly applied to a field of bacteria growing on a Petri dish (Yates *et al*., 2006). Previous antimicrobial studies on the resin have only collected categorical data (Bacteriocidal, Bacteriostatic, or No Effect) and have not reported relevant nominal data, such as determining the level of the effect compared to a control (Yates *et al*., 2006). Previous studies have also neglected the possibility that the resin may have a probiotic effect and actually promote growth of certain bacteria strains.

Chemical characterization of resin. Most research on *S. verticillata* resin has focused on use of Fourier transform infrared spectroscopy (FTIR) to characterize resins of extant and fossil conifers. FTIR spectroscopy is an effective method for chemotyping, or chemical fingerprinting, the resin and has been used successfully to chemotype *S. verticillata* resin, other plant resins, and Baltic amber (Tappert *et al*., 2011; Wolfe *et al*., 2009). The Baltic shoulder (the broad shoulder between 1200 and 1300 cm^{-1}) was a common feature of the FTIR spectra of resin from *S. verticillata* and Baltic amber, but was either partially expressed or missing from all other

extant conifers tested (Wolfe *et al.*, 2009). Baltic amber had both an ether soluble fraction containing primarily terpenes and their esters, whereas the insoluble fraction consisted primarily of communic acid and communol (Wolfe *et al*., 2009; Mills *et al*., 1984).

NMR spectroscopy is used to provide detailed physical, chemical, and structural information about molecules by using resonant frequencies of the nuclei present in the sample (Rabi *et al*., 1938; Lopez *et al.*, 2016; Martin-Pastor *et al*., 2016). Many isotopes can be used for NMR analysis, with ^{1}H and ^{13}C NMR being used most commonly (Martin-Pastor *et al*., 2016), and NMR spectroscopy is routinely required for confirmation of new compounds (Andrikopoulos, 2002). NMR has been used successfully in previous research to characterize plant resins and oils of angiosperms and gymnosperms, amber, and latex (Martin-Pastor *et al*., 2016; Megeressa *et al*., 2015; Dghim *et al*., 2015; Lopez *et al.*, 2016; Tappert *et al*., 2011).Hydrogen is highly abundant in biological systems so ^{1}H NMR can be used to characterize complex matrices (Lopez *et al*., 2016). Conversely, ^{13}C NMR can be used because its relative low abundance in nature, compared to ^{12}C, yields sharper signals and makes the spectrum appear less crowded than ^{12}C (Lopez *et al*., 2016). Combination of the two and analysis by Heteronuclear Multiple Quantum Coherence (HMQC) analysis confirms presence of chemical classes.

Previous research has successfully used pyrolysis GCMS to aid in characterizing plant resins similar to *S. verticillata* resin's appearance and physical characteristics, such as resins from the rubber tree (*Hevea brasiliensis*) (Agrawal *et al*., 2009; Liggieri *et al*., 2004). Because pyrolysis GCMS is commonly used by chemists to separate complex mixtures and to identify mass to charge ratios of a sample's components, there is a vast library available for identifying

common compounds known to be present in other resins. The technique was also used to characterize linkages in Baltic amber, a substance believed to have been derived from *Sciadopitys* or close relative (Tappert *et al*., 2011; Wolfe *et al*., 2009).

Because the resin may contain novel and/or beneficial products, further chemical characterization is needed in order to ascertain if the resin of *S. verticillata* or its bioactive component(s) can to be developed for use in agriculture. The overall goal of this research was to evaluate resin from *S. verticillata* as a potential antimicrobial source. The objectives of the first portion of this study were to: 1) identify volatile compounds present in resin of *S. verticillata* and determine their antimicrobial activities; and 2) determine effect of season on activity of *S. verticillata* resin against key bacterial species. This study is the first known attempt to quantify the seasonal effect of resin from *S. verticillata* on bacteria and to use differences in seasonal resin chemistry detected by gas chromatography mass spectrometry (GCMS) to identify the principal bioactive components responsible for the effect. The specific objectives of the second portion of the study were: 1) to compare untreated resin with resins that have been treated for use in bacterial assays (autoclaved) and those that have been lyophilized for further chemical studies (FTIR); 2) to further characterize chemical groups present in the resins (NMR and pyrolysis GCMS); and 3) to determine diversity of resin chemistry within the species (six individual trees) and compare to a previously uncharacterized conifer species (*Abies fraseri*). This study is significant in that *S. verticillata* is a rare and understudied plant that may produce novel and/or beneficial products. The research presented here was designed to provide additional information on the chemistry of the complex resin with particular attention to compounds that affect the growth of plant pathogenic and food borne bacteria.

CHAPTER 2: Methods

Microorganisms and cultures. Seven bacteria, including Gram-positive (G^+) and Gram-negative (G^-) species, were used in this study. Plant pathogenic bacteria were selected from the collection of B. H. Ownley, University of Tennessee. Species used were *Erwinia amylovora* (Enterobacteriaceae) (UTBO# E9), *Xanthomonas perforans* (Lysobacteraceae) (UTBO# SB1), *Agrobacterium tumefaciens* (Rhizobiaceae) (UTBO# C58), and *Pseudomonas syringae* (Pseudomonadaceae) (UTBO# 268). The soilborne plant commensal/human pathogen *Bacillus cereus* (Bacillacae) (CB# 154869), the beneficial *Pseudomonas fluorescens* (Pseudomonadaceae) (CB# 155255), and the human pathogen/commensal *Escherichia coli* (Enterobacteriaceae) (CB# 155068) were purchased from Carolina Biological Supply (Burlington, NC).

Resin sources. All resin used in the microbial portion of this study was collected from a single source tree grown in full sun at Laurels Nursery (Elizabethton, TN) (Figure 4). The tree was propagated by stem cutting from a tree purchased in Canby, OR in 1990. The tree was fertilized twice a year using a granular (10N-10P-10K) fertilizer applied by hand to the soil surface at the tree's drip-line. No pesticides were applied during the study period or in the six prior years. The tree was not irrigated.

Figure 4. *Sciadopitys verticillata* used as primary resin source. Tree (LN) used as primary resin source for the antimicrobial component of this study.

For the chemical characterization portion of this study, six well-established *S. verticillata* located in eastern Tennessee were used as resource trees for resin collection and were assigned a two letter designation that was used throughout the study as identifiers in data collection and analysis; the two letter designations used in Yates *et al*., 2006 are retained for trees that were used in both studies. These two letter designations are also used in some accompanying figures and tables (Example: Laurels Nursery tree = LN) (Table 1). The two trees in Elizabethton, TN (LN and VA) were located approximately 1.5 km apart and were cuttings from the same parent tree. Laurel's Nursery, approximately 20 km from Elizabethton, has an elevation 130 m higher than the city. Elevation and the middle cloud forests at LN and FL are consistent with the primary *S. verticillata* populations in Japan (Kawase *et al*., 2010).The two trees in Johnson City, TN (HC and VA) are located approximately 12 km from the Elizabethton trees and receive similar average precipitation, but the sites have warmer average temperatures due to their lower elevation. Two trees were located at the University of Tennessee (Knoxville, TN); WG was container grown and maintained in a climate controlled greenhouse, and the UT tree was located

in the University of Tennessee Gardens. At the end of the study, WG was donated to the University of Tennessee Forest Resource AgResearch and Education Center, Oak Ridge, TN and remains as part of the conifer collection. Samples were also collected from Fraser fir (FF), Norway spruce (NS) and white pine (WP) grown at Laurel's Nursery. Mean monthly rainfall, temperature, and day length during study period for cities closest to the collection sites are shown in the Table A.1.

Table 1. Resource trees for resins.

		TN City Resin Collected	**Location**	**Year Planted**	**Source**	**Sun**	**Elevation** (Meters)
LN	*Sciadopytisverticallata*	Elizabethton	Laurel's Nursery	1990	Cutting from tree purchased from Canby, OR	Full Sun	615
VA	*Sciadopytisverticallata*	Johnson City	Veterans' Administration Hospital - Mountain Home	1940s	Japan	Full Sun	465
HC	*Sciadopytisverticallata*	Johnson City	Personal collection of Hugh Conlon	1990	Blue Sterling Nursery, Bridgeton, NJ	Partial Shade	465
FL	*Sciadopytisverticallata*	Elizabethton	Personal collection of Foster Levy	1990	Same as LN	Full Shade	579
UT	*Sciadopytisverticallata*	Knoxville, TN	University of Tennessee Gardens	unknown	unknown	Partial Shade	270
WG	*Sciadopytisverticallata* cv Wintergreen	Knoxville, TN	University of Tennessee North Greenhouse	Container -grown	Willow Ridge Gardening and Landscaping Center, Oak Ridge, TN	greenho use	270
FF	*Abies fraseri*	Elizabethton	Laurel's Nursery	2004	Roan Mountain, TN	Full Sun	615
WP	*Pinus strobus*	Elizabethton	Laurel's Nursery	2006	TN Dept. Forestry	Full Sun	615
NS	*Piceaabies*	Elizabethton	Laurel's Nursery	2002	NM Dept. Forestry	Full Sun	615

Resin extraction and preparation. Preliminary studies were conducted to determine solubility of the resin. Resin was extracted from freshly cut ends of stems or bundles of 8-12 needles of *Sciadopitys* placed in approximately 0.5 mL of sterile deionized water for about one hour (Figure 5). Resin suspensions were consolidated in pre-weighed tubes and centrifuged at 10000 rpm for five minutes and supernatant was removed. Resin pellets were extremely viscous; therefore, to facilitate pipetting, resins used for microbial testing were re-suspended in distilled water (1:2 v/v). Resin suspensions were autoclaved twice at 115 °C for 40 minutes to ensure that

any adverse effects could not be attributed to contaminating organism(s). In preliminary tests, autoclaving did not affect antibacterial activity of the resin. Resin was collected in summer (June/July) and winter (February/March) of 2013 and stored at -20 °C. For most experiments, resin was tested within 72 hours of collection, but resin stored for 6 months was used in some tests.

Figure 5. ***Sciadopitys verticillata*** **resin extraction.** Fresh cut stems and leaves (needles) were submerged in sterile water for approximately one hour. Resin quickly formed a pellet.

Gas chromatography-mass spectrometry compound identification of resin. Resin suspensions were centrifuged, and supernatant discarded. The pellet was frozen at -20 °C for 48 hours and then lyophilized for 72 hours. Samples were prepared by dissolving the lyophilized resin pellet in dimethyl sulfoxide (DMSO) (100000 ppm). Once dissolved, samples were diluted to a concentration of 200 ppm with optima grade ethyl acetate. Diluted samples were analyzed using an Agilent Technologies 7890B Gas Chromatograph (Santa Clara, CA) coupled to a 5977Agilent Mass Selective Detector. Sample (1 µL) was delivered into the 250 °C splitless inlet

by autosampler, where a mobile phase of ultra-high purity helium gas carried the sample along the 30 m x 0.25 mm (250 micron) column. The ramp was first held at 50 °C for 0.5 minutes before increasing to 300 °C at a rate of 20 °C/min with a two-minute bake-out at 325 °C. Peaks were identified using MassHunter software equipped with the NIST02 Library.

Peak area percentages were calculated, and data analyzed with a Wilcoxon Signed rank test at P = 0.05. This test is used for the non-parametric format of paired t-tests due to non-normality of data. All data were analyzed for significance with SAS 9.4 TS1M3 for Windows (SAS Institute Inc. Cary, NC).

Resin antibacterial activities. Bacterial suspension cultures were prepared in Difco™ Nutrient Broth (NB) (Becton, Dickenson, and Company, Le Point de Claix, France) and incubated at 30 °C. After 24 hours, the suspension was centrifuged at 10000 rpm for five minutes. Supernatant was removed; the pellet was re-suspended in fresh liquid NB, and diluted to 75% (±2.5%) transmittance using a Turbidimeter™ (Biolog Inc., Hayward CA).

All treatments were incubated in honeycomb microplates (Growth Curves USA, Piscataway, NJ). Bacterial suspension (100 µL) and NB medium (100 µL) were added to test wells. There were four resin treatments [0 (control), 25, 50, and 100 µL resin]; deionized water was added to bring the final volume to 300 µL. Bacteria were incubated with constant shaking for 24 hours at 30 °C in a Labsystems Bioscreen C (Oy Growth Curves Ab Ltd, Raiso, Finland) microtiter plate reader. Suspension cultures were serially diluted in sterile water and the 10^{-3} to 10^{-8} dilutions were plated onto NB medium with a microplating technique, in which nine 10 µL drops of the bacteria/resin suspensions were pipetted, onto one Petri dish (Dee *et al*., 1995). Inoculated plates were stored either at room temperature or at 30 °C (*E. coli* only). The number of colonies in each

drop were counted after 1-2 days, depending on bacterial growth rate. Each microplate well served as a replicate, and each treatment was replicated three times. Three dilution series were made from each well, and for each dilution, bacteria were counted in the nine subsamples previously described. Experiments were not repeated for bacteria for which there were no apparent effects in the first trial; others were repeated twice.

All bacteria (except *Pseudomonas syringae*) were tested using resin collected in both summer and winter. The GCMS data were collected on resins that were stored for a 6-month period between the summer and winter collections; this allowed samples to be processed and analyzed simultaneously. Selected pathogens were tested with resin collected in the summer and stored for 6 months.

Data analyses were conducted with SAS (Version 9.4 TS1M3) for Windows (SAS Institute Inc. Cary, NC). Microbial population data was analyzed using mixed model ANOVA. Experiments were arranged in a randomized complete block design (winter data) or completely randomized design (summer data). Data were rank transformed because the ANOVA assumptions of normality and equal variance were violated in untransformed data. Post hoc multiple comparisons among treatments were conducted with Tukey's adjustment at $P = 0.05$.

Antimicrobial activity of identified compounds. The commercially available primary volatiles (α-pinene and β-pinene) identified in the resin were tested for activity against *B. cereus*, the most sensitive of the test bacterial species. Autoclaved diffusion discs were saturated in filtered (45-µm filter) suspensions of α-pinene (Aldrich Chemical Inc., Milwaukee, WI). Excess liquid was removed by holding discs with forceps and gently shaking. Four concentrations were tested (8, 16, 32, and 100%). One mL of bacterial suspension (prepared as described above) was

sprayed onto Nutrient Agar. After ten minutes, diffusion discs were placed on the medium. Bacteria were incubated for 48 hours, and then inhibition zones were measured.

Additional antimicrobial trials with α-pinene were performed as described above for resin except that physiological levels of α-pinene solution, which approximated concentration in the resin treatment, were used. Bacterial growth at 30 ºC was monitored as increased absorbance at 420-580 nm (Microbiology Reader Bioscreen C, Growth Curves USA, Piscataway, NJ); absorbance was measured every 30 min for 8 hours. Experiments were repeated twice. In order to fully access antimicrobial activity, concentrations of α-pinene that were approximately 1000× concentrations in the resin were used. Final concentrations in the microplate wells were 7.2 mg/mL, 14.4 mg/mL, and 28.8 mg/mL. Bacterial populations were plated and counted as described above.

Chemical characterization of resin. Analysis was performed on resins that were untreated (FTIR), autoclaved (FTIR), and lyophilized (FTIR, NMR, and pyrolysis GCMS). Lyophilized resin was prepared by resin extracted from freshly cut ends of stems or bundles of 8-12 needles of *S. verticillata* placed in approximately 0.5 mL sterile deionized water for approximately one hour. Resin suspensions were consolidated in pre-weighed tubes and centrifuged at 10000 rpm for five minutes. Supernatant was removed. Resin pellet was frozen at -20 °C for 48 hours then lyophilized for 72 hours. Autoclaved resins were prepared from resins that were collected and processed as described above except that the resin was re-suspended in water. Suspensions were autoclaved at 115°C for forty-five minutes.

Nuclear magnetic resonance. NMR spectra were measured on a latex sample (LN) prepared by dissolving 105 mg of lyophilized latex in 750 ml of d6-dimethylsulfoxide and

filtering into an NMR tube through a small piece of Kimwipe in a Pasteur pipet. ^{1}H and ^{13}C spectra were carried out on a Varian 400-MR spectrometer equipped with a broadband probe operating at 399.78 MHz for proton and 100.54 MHz for carbon. Double quantum filtered (DQF) COSY spectra were acquired over 256 increments, with 8 scans per increment. Gradient heteronuclear multiple quantum coherence (gHMQC) spectra were acquired over 512 increments with 32 scans per increment giving a spectrum size of 1024 x 1024. A 90^{o} pulse with a pulse delay of 1.5 seconds, and an acquisition time of 0.15 seconds. All spectra were processed using MNova software. The HMQC spectra were processed with MNova using a t1 noise reduction algorithm, a third order Bernstein polynomial baseline fit, and Lorentz-to-Gauss apodization using an exponential function of -0.5 Hz and a Gaussian function of 15 Hz in the F2 direction and an exponential function of -10.0 Hz and a Gaussian function of 100 Hz in the F1 direction. All spectra were referenced to the residual DMSO signal at 39.5/2.5 ppm. Two-dimensional analytical technique Heteronuclear Multiple Quantum Coherence (HMQC) was used to analyze samples for groupings of chemical classes present in the resin.

FTIR evaluation of resin. Resins (LN) used for FTIR evaluation of autoclaving and lyophilization were processed without additional treatment, lyophilized, or autoclaved as described above. Resin samples were placed onto the diamond sample window and scanned (650–4000 cm^{-1} spectral range, 8 cm^{-1}spectral resolution, 32 scans per spectrum) using a Frontier EGA/PY-3030 D pyrolyzer. Separations of the pyrolysis vapors were carried out on a Perkin Elmer Clarus 680 gas chromatograph with an Elite 17 MS capillary column (30 m 9 0.25 mm ID 9 0.25 μm film thickness). The split ratio was 80:1with helium as the carrier gas (1 mL/min). Oven temperature for the gas chromatograph was held at 50 °C for 4 min and then ramped to 280

°C (5 °C/min). Spectra used for PCA included ten independently expressed and scanned subsamples. The ATR pressure anvil was not needed on fluid samples, but was used on resin pellets to ensure sufficient contact with the diamond window. Resins from other conifers were extracted in water and tested as described for the treatment comparisons.

Pyrolysis gas chromatography mass spectrometry of resin. In this study resin from all six source trees were collected in summer (2014) and lyophilized as described above. Three subsamples (300 μg) were weighed in stainless steel cups and pyrolyzed using a Frontier EGA/PY-3030 D pyrolyzer. Separations of the pyrolysis vapors were carried out on a Perkin Elmer Clarus 680 gas chromatograph with an Elite 17 MS capillary column (30 m, 0.25 mm ID, 0.25 μm film thickness). The split ratio was 80:1with helium as the carrier gas (1 mL/min). Oven temperature for the gas chromatograph was held at 50 °C for 4 min and then ramped to 280 °C (5 °C/min). Peaks representing individual pyrolysis degradation products were identified using a Perkin Elmer Clarus SQ 8 GC mass spectrometer. For comparison between individual resin source trees, spectra were visually analyzed for differences in peak location and intensity.

Multivariate analyses of the resin FTIR spectroscopy and pyrolysis–GC–MS data were performed using the CAMO Unscrambler (version 8.0) software. Principal component analysis (PCA) was performed on the spectral data to observe differences and groupings between the sample sets. Pyrolysis–GC–MS chromatograms were analyzed in an analogous manner. When PCA groupings between the sample sets indicated a difference in samples, loadings graph was used to identify the principle component being compared.

CHAPTER 3: Results and Discussion

Physical characteristics of resin. The resin is white and its uneven suspension in the aqueous environment precluded photometric monitoring of bacterial population growth. The resin formed a dense pellet in non-polar solvents (toluene and hexane) (Figure 6). The polar solvents acetone, ethanol, and methanol partially dissolved the resin; DMSO also dissolved resin and was used as the first solvent in chemical analyses. However, the concentrations of DMSO required to dissolve the resin were bacteriocidal and could not be used in antimicrobial trials (Hoerr *et al*., 2016). Water was chosen as the solvent for antimicrobial testing because it prevented the resin from dehydrating and becoming brittle, it also facilitated cold storage of the resin, and the stored resin could be re-suspended by vortexing. After lyophilization (one week), the resin was brown, sticky, and extremely viscous. Drying lyophilized resin in an oven at 120 °C for six hours yielded a yellow liquid.

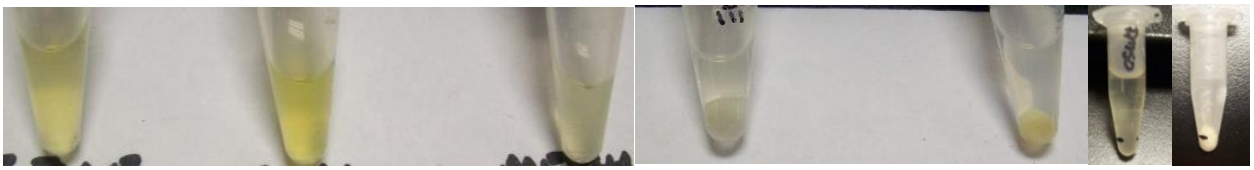

Figure 6. Solubility of resin in selected solvents. Seven common solvents were tested to determine the best solvent for use in the chemical characterization and bioactivity components of this research. From left to right: acetone, ethanol, methanol, toluene, hexane, DMSO, and water.

Gas chromatography mass spectrometry analysis of resin. Eighteen volatilized compounds were tentatively identified in lyophilized resin (Table A.2). Seventeen of the identified compounds are classified as terpenes $(C_5H_8)_n$, with the remaining compound β-ionone

being a norisoprenoid. It was not surprising that the aromatic resin of *S. verticillata* contained high concentrations of terpenes, because terpenes are aromatic compounds that often have protective functions as either deterrents or attractants of microbes and insects in many plants, including pines. Terpenes are major constituents of essential oils, fragrances, and medicines. Due to their lipophilicity, terpenes insert into cell membrane, causing membrane changes in porosity, which in turn affect transport (Dhar *et al*., 1995; Maskovic *et al*., 2013). Other white plant resins also contain mixtures of terpenoids such as cis-1,4-polyisoprene (rubber) that give latex its white color, phenolic compounds (tannins, lignins, and flavonoids), and alkaloids (morphine) that are toxic to insects and vertebrates, and include various proteins, minerals, and carbohydrates(Agrawal *et al*., 2009; Langenheim, 2003). Of the identified compounds, only three compounds represented>5% of the total of peak areas. When added, these three compounds account for approximately 95% of the peak area of resin volatiles.

In both resins, the terpene 1R-*α*-pinene was the primary component and comprised 73.5% of resins collected in the summer or 82.0% of resins collected in the winter of the total volatiles (Table 2).α-pinene is a common antimicrobial lipophilic monoterpene found in several essential oils. It is commonly used in the fragrance industry, and in medicine as a topical antiseptic, a dietary additive to increase mental focus and energy, and as a bronchodilator for asthma patients (Dhar *et al*., 2014; Bozin *et al*., 2007; Iscan *et al*., 2007; Dadalioglu *et al*., 2004). In pine, α-pinene is found as enantiomers (1S,5S)- or (−)-α-pinene or (1R,5R)- or (+)-*α*-isomer (Lis-Balcnina *et al*., 1999). α-pinenes are reactive hydrocarbons prone to skeletal rearrangements, causing antimicrobial activity by interfering with cell membrane form and/or function (Dhar *et al*., 2014; Bozin *et al*., 2007; Lis-Balcnina *et al*., 1999).

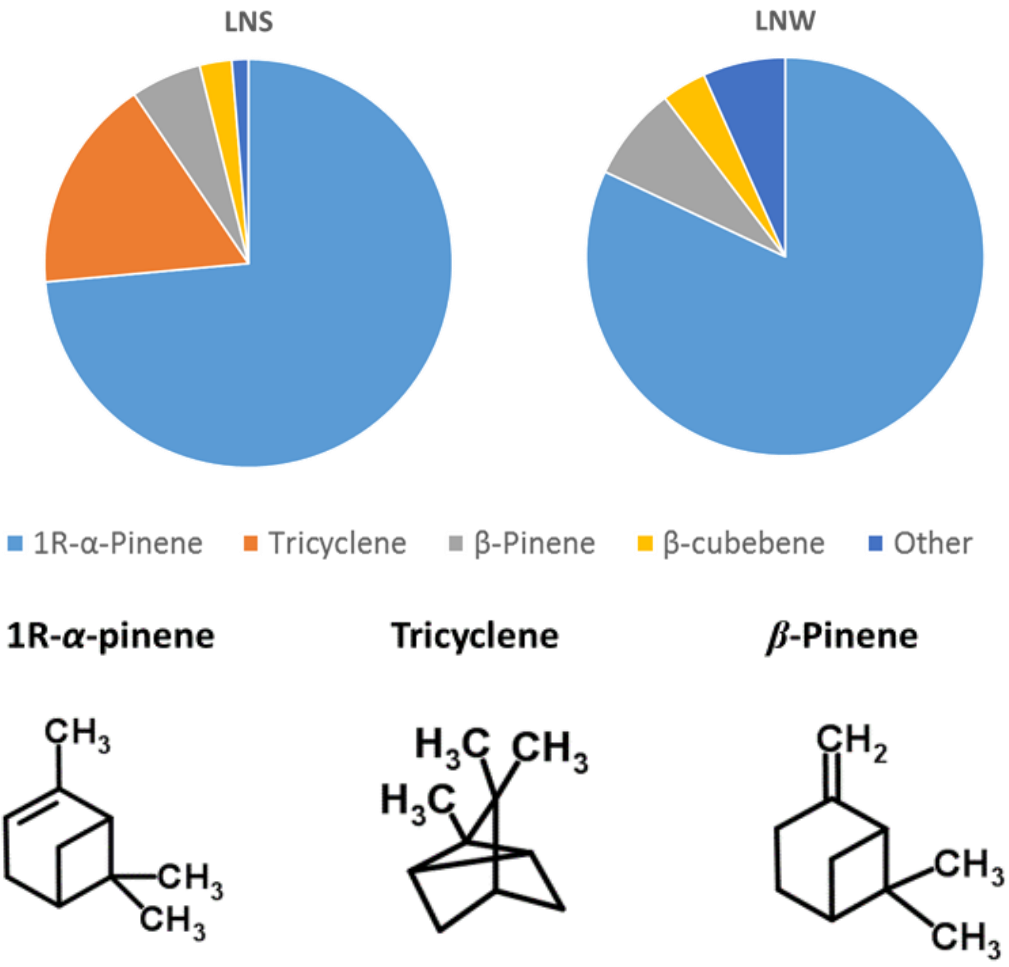

Figure 7. Volatile resin compounds identified in GCMS. Volatiles identified using GC-MS and their relative abundance in the resin were compared seasonally. The three most abundant volatiles in the resin and their structures are shown.

Table 2. Compounds identified in resin by GC-MS. Resin compounds identified using the MassHunter software to search the NIST02 library of mass spectra and listed by percent of total peak areas (Largest to smallest). Not Present (NP) indicates that the compound was not identified in the resin sample.

Chemical Name	Retention Time	Summer		Winter	
		Score	% Peak Area	Score	% Peak Area
1R-α-pinene	5.474	92.73	**73.552**	92.35	**82.003**
Tricyclene	5.399	88.18	**16.977**	**NP**	**0.000**
β-pinene	5.794	81.17	**5.613**	83.4	**7.656**
β-cubebene	9.222	92.4	**2.540**	77.36	**3.635**
D-limonene	6.132	87.84	**1.634**	88.21	**1.784**
Camphene	5.600	81.46	**0.816**	80.25	**0.789**
Contaminant (Silica gel)	10.189		**0.796**		**0.900**
3 7 α-terpinyl propionate	8.306	78.23	**0.432**	80.23	**0.579**
β-cubebene	8.907	82.07	**0.388**	84.98	**0.541**
β-cubebene	8.844	84.68	**0.384**	86.65	**0.586**
1-Naphthalenol	9.405	76.91	**0.316**	78.49	**0.472**
γ-Cadinene	8.627	84.76	**0.171**	88.42	**0.267**
Caryophyllene	8.867	87.05	**0.113**	88.26	**0.195**
Copaene	8.558	81.98	**0.110**	79.42	**0.159**
β-ionone	9.954	71.69	**0.104**	74.25	**0.181**
1,5,9,9-tetramethyl-1,4,7-cycloundecatriene	9.073	70.43	**0.045**	**NP**	**0.000**
7 a-terpinyl propionate	9.588	62.92	**0.041**	69.18	**0.124**
Tetracyclo[5.3.1.1(2,6).0(4,9)]	9.845	60.52	**0.033**	**NP**	**0.000**
γ-Cadinene	9.067	NP	**0.000**	93.00	**0.128**

Ability to cross membranes, including the brain barrier, makes pinene a potential drug delivery compound (Dhar *et al*., 2014). Because 1R-α-pinene, the major detected compound in our resins, is commercially available, it was used for microbial testing.

The second most abundant compound in the resin collected in the summer was tricyclene (1,7,7-trimethyl-Tricyclo[2.2.1.0(2,6)]-heptane), comprising 17% of total peak areas (Table 2) (Figure 7). Tricyclene was not detected in winter-collected resin. Tricyclene is a crystalline saturated tricyclic terpene hydrocarbon ($C_{10}H_{16}$) found in crude α-pinene (Nikolic *et al*., 2009). Tricyclene has more activity against G^+ than G^- microorganisms (Rajaian *et al*., 1999). Tricyclene was not commercially available and so was not tested for antimicrobial activity.

Volatiles from summer- and winter-collected resins were remarkably similar given our preliminary observation that antibacterial activity against *E. coli* was greater in the winter. Resins from both collection seasons contained β-pinene, 5% - 8% of volatiles. β-pinene is a colorless liquid monoterpene and is one of the most abundant compounds released by forest trees (Geron *et al*., 2000). β-pinene is soluble in alcohol, but not water (Mahajan *et al*., 2016).β-pinene has antioxidant activity, is a membrane stabilizer, and can lessen the effect of environmental stress and heavy metals in plants (Mahajan *et al*., 2016; Singsaas, *et al*., 2000; Loreto *et al*., 2001). Antimicrobial activity of β-pinene was not tested at physiological levels because of its relatively low concentration compared to its structural isomer, 1R-α-pinene (11- to 13-fold less) and its relative inactivity. Data analyses for all microbial studies are shown in Tables A.3-A.16.

FTIR evaluation of resin collected for two years. For both years, temperature and rainfall were greater in the summer than in the winter. The winter of 2014 was warmer than the winter of 2013 by almost 2°C, and had approximately 1.5 cm more precipitation. Summer

temperatures were within 1 °C in the two years, but rainfall in 2013 was almost twice 2014. Principal component analysis was used to determine the effect of season and year on the chemical composition of the resins. There were no differences when resin collected in the same year (Figure A.3) or resins collected in the same season in different years were compared (Figure A.4).

Stimulation of growth. Population counts of three species of bacteria increased in treatments containing resins. Resin treatment increased the population size of *X. perforans* between 27% - 277% (Figure 8). While all the summer resin treatments increased growth, there were no differences among concentrations of resin, suggesting that there is no advantage to using a higher concentration of resin to promote growth of *X. perforans*. Although *X. perforans* is a plant pathogen that causes economically costly blights, cankers, and bacterial leaf spot, some *Xanthomonas* species are utilized commercially to produce xanthan gum, an exopolysaccharide added to foods, petroleum products, and cosmetics (Barrere *et al*., 1986).

When compared to the control (0 µL resin), the lowest concentration of resin collected in the summer (25 μL) had no significant effect on growth of *P. fluorescens*, but growth increased with resin treatments collected in the summer that had been stored for 6 months or winter resin (72% and 141%, respectively) (Figure 9). Treatments containing moderate amounts of resin (50 μL) increased growth significantly more than the low resin treatments at all collection times. There were no differences in the patterns of inhibition between resin collected in the summer and

immediately tested and those stored for 6 months, but the magnitude of the increase in the numbers of bacterial cells was greater in the fresh resin. Increased numbers of bacteria in treatments with high amounts of resin collected in the summer and immediately tested (19-fold increase over control) were greater than the summer-stored and winter-fresh resins (6-fold and 4-fold increases over no resin controls respectively). Although *P. fluorescens* is a food contaminant, it is also considered a beneficial bacterium due to its ability to protect plant roots from parasitic fungi such as *Fusarium* or *Pythium*, as well as some phytophagous nematodes, and some strains have been used as biological controls against fire blight caused by *E. amylovora* (Haas *et al*., 2003). Some strains of *P. fluorescens* can utilize α-pinene as a carbon source (Cheng *et al*., 2013).

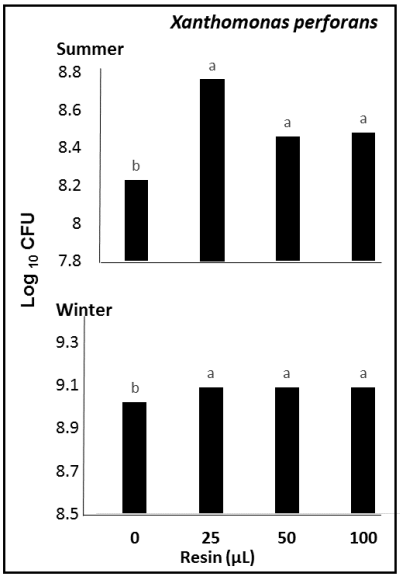

Figure 8. Antimicrobial activity of *Sciadopitys verticillata* resin tested in summer and winter against *Xanthomonas perforans.* Within season of collection, bars appearing with the same letter are not different ($P < 0.05$).

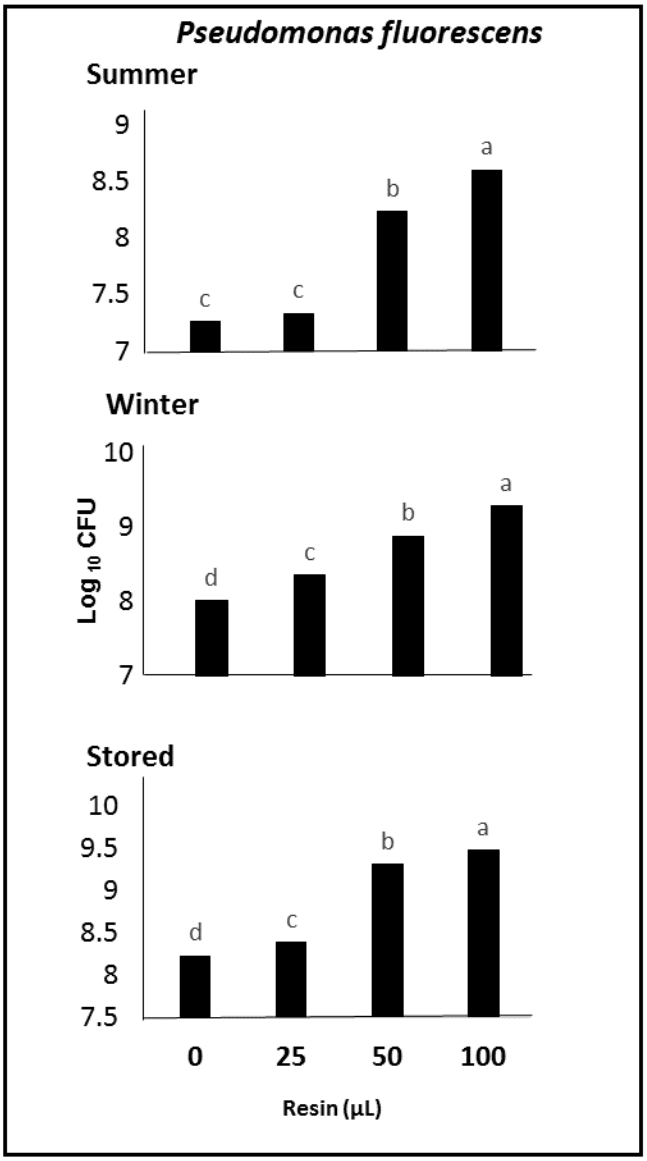

Figure 9. Antimicrobial activity of *Sciadopitys verticillata* resin collected in summer, winter, or stored for 6 months against *Pseudomonas fluorescens*. Within season of collection, bars appearing with the same letter are not different ($P < 0.05$).

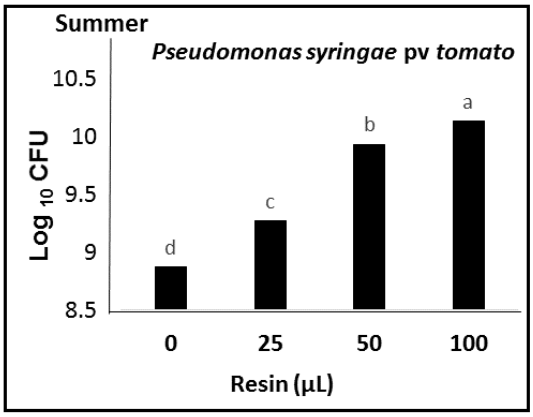

Figure 10. Antimicrobial activity of *Sciadopitys verticillata* resin collected in summer against *Pseudomonas syringae.* Bars appearing with the same letter are not different ($P < 0.05$).

Because *P. fluorescens* was able to use the resin as a food source, it was necessary to determine if plant pathogenic bacterial species were also able to utilize it. Winter-collected resin was used to determine bioactivity against *Pseudomonas syringae pv. tomato*, a pathogen that causes economic loss in tomatoes (Wageningen *et al*., 2004) (Figure 10). Populations of *P. syringae* increased in a manner similar to *P. fluorescens* validating concerns that the resin would not be a viable biopesticide option on crops such as tomatoes that are highly susceptible to pathogens in the genus *Pseudomonas*.

Microbial growth inhibition (Human health). All other bacteria tested were inhibited by treatment with resin collected from *Sciadopitys*, including those that affect human health. All resin treatments reduced populations of *Bacillus cereus* between 42% - 86% of control, but there were no significant differences among the different concentration levels indicating that there was no advantage to using a higher concentration of resin (Figure 11). There was a reduction in numbers of cells between the low and high treatments of winter-collected resin, with the high

treatment reducing growth an additional 44%. Efforts of control *B. cereus* are critical within the food industry because tainted agricultural products have caused both emetic and diarrheal syndrome types of food poisoning (Schoeni *et al*., 2005).*Bacillus* was the sole G^+ bacterium tested and these bacteria are more sensitive to tricyclene than G^- bacteria (Meccia *et al*., 2009). Antimicrobial activity in winter is not due to tricyclene since it is not present. Control *B. cereus* is difficult because it spreads easily by spores that can withstand boiling, and are not easily killed by alcohol. Indeed, spores of *B. cereus* have been recovered from distilled liquors and alcohol-soaked swabs and pads in numbers large enough to cause infection (Hsueh *et al*., 1999).Resin of *S. verticillata* is a potential source of future antimicrobials, seed protectants, or food packaging to protect against *B. cereus*.

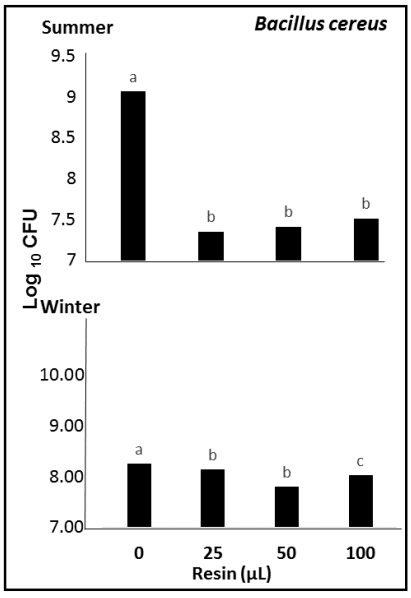

Figure 11. Antimicrobial activity of *Sciadopitys verticillata* resin collected in summer or winter against *Bacillus cereus*. Within season of collection, bars appearing with the same letter are not different ($P < 0.05$).

When compared to the control treatment, all resin treatments, regardless of season collected, or whether the resin was freshly collected or stored in refrigeration, significantly reduced growth of *E. col* (Figure 12). The low resin treatments reduced cell count by 7% - 30%. The higher resin concentration treatments controlled growth significantly better than the low resin treatments. Increased resin concentrations decreased growth in summer-stored and winter-fresh resins; however, there were no significant differences in the antimicrobial activity among treatments of summer-fresh resin treatments. The possibility exists that differences in the bioactivity of the summer resin used fresh, and used after being stored may be due to changes caused by exposure to cold since summer-stored and the winter-fresh were similar in bioactivity.

Microbial growth inhibition (Plant Pathogens). When compared to control, the low and moderate resin treatments significantly decreased growth of *A. tumefaciens* (Figure 13). There were no significant differences in the control provided by the low summer resin treatments, which yielded a 49% reduction in number of colony-forming units (CFU) and the moderate treatment that had 46% fewer CFUs. The low and moderate winter resin treatments did not differ significantly, nor did the moderate treatments differ from the high. There is no advantage to using the higher rate to control *A. tumefaciens*; however, there was much better control using summer resin (-49%) than winter resin (-25%). *Agrobacterium tumefaciens* integrates some of its own DNA (t-DNA) into the host genome, resulting in tumors and changes in plant metabolism and causing great economic losses (Lang *et al*., 2014). Plant tissues transformed by t-DNA accumulate opines, which the bacterium uses as growth substrates. In the tumor, opines are trapped by ligand-binding, thus constructing an opine-enriched niche that confers a selective advantage to the pathogen (Lang *et al*., 2014). Resin from *S. verticillata* may

be a candidate for development as a biological control against *A. tumefaciens* at low levels, but not at high levels since there appear to trigger utilization of the resin.

Numbers of *Erwinia amylovora* were reduced in all resin treatments regardless of season collected, or whether the resin was freshly collected or stored at low temperature (Figure 14). When compared to control treatment, treatments containing low resin significantly reduced populations of *E. amylovora* by 19% - 34%, with summer-fresh resin providing the least control. The high resin concentration treatments had populations significantly lower than the low resin treatments. Treatments containing moderate resin reduced population by 47% - 67% and high resin treatments reduced growth by 50% - 72%. There was no advantage to using the concentrations greater than 50 μL to control *Erwinia*. At 1500 μg/ml, α-pinene and β-pinene reduced growth of *Erwinia amylovora* (Scortichini *et al*., 1991). Because *P. fluorescens* (stimulated by the resin) is a biological control agent for *E. amylovora* (inhibited by the resin), use of *S. verticillata* resin in combination with *P. fluorescens* should be investigated.

Resin from *Sciadopitys* was inhibitory to *B. cereus, A. tumefaciens, E. coli, and E. amylovora,* but populations increased when both species of *Pseudomonas* and *X. perforans* were grown in the presence of this resin. *Erwinia* and *E. coli* are both members of the Enterobacteriaceae and are the most closely related of the bacterial species tested in this study. Of all the plant pathogens tested, exposure of *Erwinia* to the resin resulted in the greatest inhibition, but inhibition was not as great as for *E. coli*. This may reflect relative amounts of plant-derived natural products in the ecological niche of each bacterium. Populations of two plant pathogens increased with resin treatment with the increase for the pseudomonads (>7.5-

fold increase) greater than that for *Xanthomonas* (> 2.7-fold increase). *Bacillus cereus* was more sensitive than *E. coli*.

Impact of α-Pinene on Growth of *Bacillus cereus*. Physiological concentrations of α-pinene in resin were calculated to approximately 71 µg/mL (low), 142 µg/mL (moderate) and 284 µg/mL (high). At these levels, there were no zones of bacterial inhibition in disc diffusion tests. In tests where bacteria growth was monitored by absorbance, allα-pinene treatments corresponding to low, moderate, or high concentrations of resin increased growth of B. cereus populations after 8 hour, with maximum growth at 12 hour (4-8 fold increase) (Figure 15).

After 24 hour of exposure, low treatment of α-pinene increased population growth by 50%, and moderate and high α-pinene treatments increased growth approximately two-fold. There were also significant differences in the treatment levels, with larger amounts of α-pinene correlating to larger populations of *B. cereus.* Utilization of pinene has been shown for other *Bacillus* species, but we think that this is the first report of the stimulation of growth of *B. cereus* by *α*-pinene. At 5 to 15 mM concentrations that are more, i.e., up to 250× those that we reported, *B. pallidus* degraded α-pinene, β-pinene, and limonene, whereas, a strain of *B. simplex* isolated from a pine-dwelling beetle, was completely inhibited by α-pinene at 8.5 µg/mL, a concentration similar to those in this study (Savithiry *et al*., 1998; Adams *et al*., 2011).

In order to determine if α- and β-pinene are active against *B. cereus*, we used the highest concentration possible in our Bioscreen C system. Data from the highest doses (28.8 mL/mL) were excluded because they altered the plastic in the honeycomb wells. Both treatments of α-pinene inhibited *B. cereus* growth (as measured by absorbance) for 16 hour (Figure 16). The low concentration treatment (25 µL) initially provided significant control (-36% at 4 hour). The high

treatment (14.4 mg/mL) had maximum inhibition (-70%) after 8 hour of exposure, which was reduced over time to a 20% reduction in growth. Growth in the two pinene treatments was different at all times (Table 3). Both concentrations of β-pinene initially gave significant control of *B. cereus* populations (62-77% reduction at 8-12 hour), but was lost by 16 hour (7-12% reduction). Neither concentration of β-pinene provided significant control of growth over the 24-hour-period.

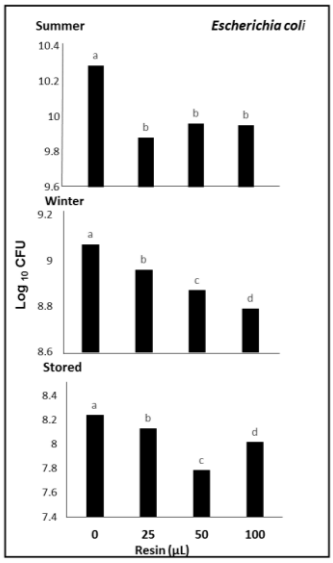

Figure 12. Antimicrobial activity of *Sciadopitys verticillata* resin collected in summer, winter, or stored for 6 months against *E. coli*. Within season of collection, bars appearing with the same letter are not different ($P < 0.05$).

Relationship of microplate absorbance values to CFU was determined for the tests with 1000x α-pinene. There was a reduction in *B. cereus* populations at low and moderate full strength α-pinene treatments as compared to controls; CFU were 21% of control in the low and

47% of control in high α-pinene treatments. The two α-pinene treatments were different from and moderate treatment reduced populations significantly better than low treatment ($P \leq 0.05$).

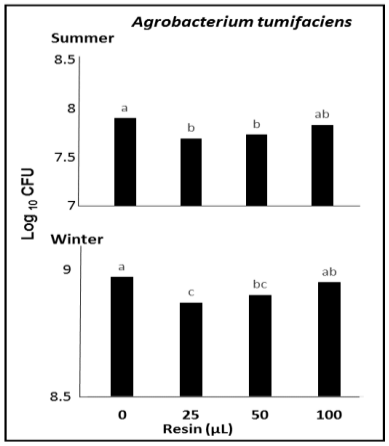

Figure 13. Antimicrobial activity of *Sciadopitys verticillata* resin tested in summer or winter against *Agrobacterium tumefaciens*. Within season of collection, bars appearing with the same letter are not different ($P < 0.05$).

The resin of *S. verticillata* is a complex blend of compounds. The stimulatory effect of the resin on the pseudomonads and the inhibitory response on the Enterobacteriaceae coupled with the presence of α-pinene as the primary volatile in the resin led to the hypothesis that α-pinene was the active component of the resin. However, antimicrobial control with α-pinene at physiological concentrations was significantly less than with the resin. In the tests on antimicrobial activity of resin, which was suspended in water, populations of *B. cereus* were reduced more than treatment with α-pinene at concentrations that were 1000x higher than in the resin, but at 14.4 mg/mL concentration, control was similar to the moderate rate of resin (42%).

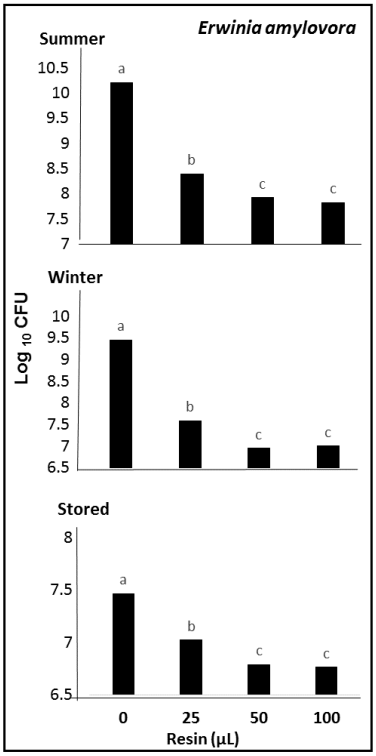

Figure 14. Antimicrobial activity of *Sciadopitys verticillata* resin tested in summer, winter, or stored for 6 months against *Erwinia amylovora*. Within season of collection, bars appearing with the same letter are not different ($P < 0.05$).

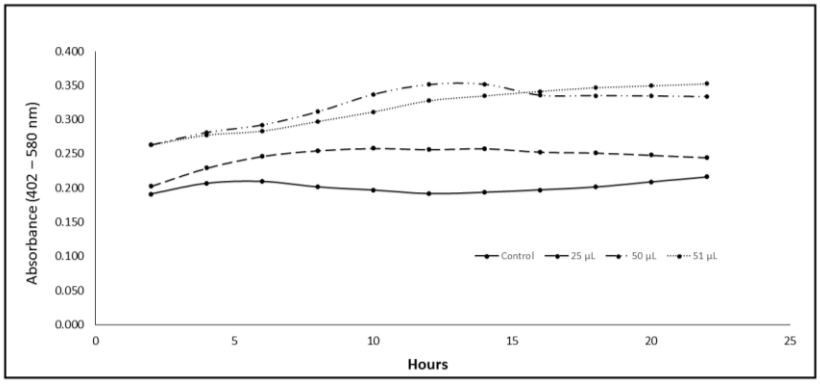

Figure 15. Growth of *Bacillus cereus* in media amended with α-pinene at levels found in resin. Absorbance of *B. cereus* suspended in concentrations of α-pinene equivalent to α-pinene levels in *S. verticillata* resin used in microbial testing.

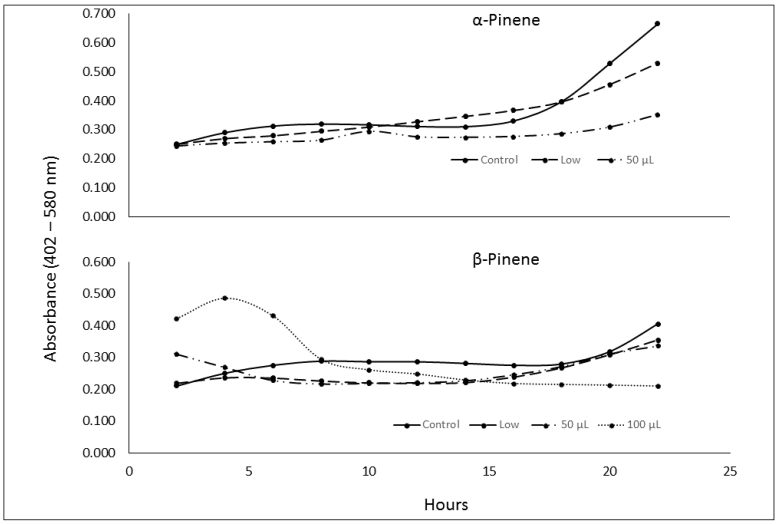

Figure 16. Growth of *Bacillus cereus* in media with varying doses of α- and β-pinene. Absorbance of *B. cereus* suspended in varying concentrations of α- and β-pinene approximately 1000x levels of the compounds in the *S. verticillata* resin suspensions used in microbial tests. Control (0 µL), low (7.2 mg/mL), and high (14.4 mg/mL).

The antimicrobial activity of the resin does not appear to be due solely to the volatiles associated with the resin, therefore additional chemical characterization of the resin is necessary before biopesticidal potential of the plant-derived resin can be fully developed; however, it should be noted that the samples used for CGMS were lyophilized and those used in the growth studies were autoclaved. Future studies with additional characterization of the resin, and testing to determine if the combination of pseudomonad biological control agents with the resin can enhance the control of plant diseases caused by bacterial pathogens.

The resin from *S. verticillata* is a complex matrix that is fully soluble only in DMSO, therefore previous reports relied on FTIR techniques which can be used with little or no sample preparation. Three analytical techniques, each with its advantages, disadvantages, and different ability to elucidate various resin components were used to further characterize the resin. Since

untreated resin from *S. verticillata* had previously been characterized by FTIR. FTIR spectroscopy was used in this research to analyze resin freshly extracted from stems or needles, lyophilized resin, and autoclaved resin (Tappert *et al*., 2011; Wolfe *et al.*, 2009). FTIR spectra of untreated resins was compared to spectra of resin that had been treated with heat (autoclaved) or lyophilized. The two treatments were necessary either for the microbial studies (autoclaved) or pyrolysis and NMR (lyophilized). Autoclaving was necessary because the resin could not be sterilized by filtration and because it eliminated potential confounding results in cell count data from non-target bacteria and fungi. Both techniques have the potential to significantly alter resin chemistry, particularly the presence of antimicrobial volatiles. Heat could also alter important non-volatile compounds, such as enzymes, that could be an effective antimicrobial component of untreated resin or sugars that may be a carbon source for the bacteria and thus be a contributor for any probiotic effect.

Nuclear magnetic resonance. NMR spectra (Figures17 and 18) had families of sharp, well-shaped lines, indicative of low molecular weight compounds. Classes of compounds tentatively identified were aldehydes, aromatics, olefins, alkoxy groups, alkyls, and carbonyls. Because the corresponding GCMS data suggested that limonene was a component of the mixture, spectra of limonene standard was compared to resin spectra (Figure A.2). The spectra remain quite complex, but the presence of limonene is suggested by comparison with the standard. HMQC analysis confirmed presence of earlier identified chemical classes and additionally ethers (Figure 19).

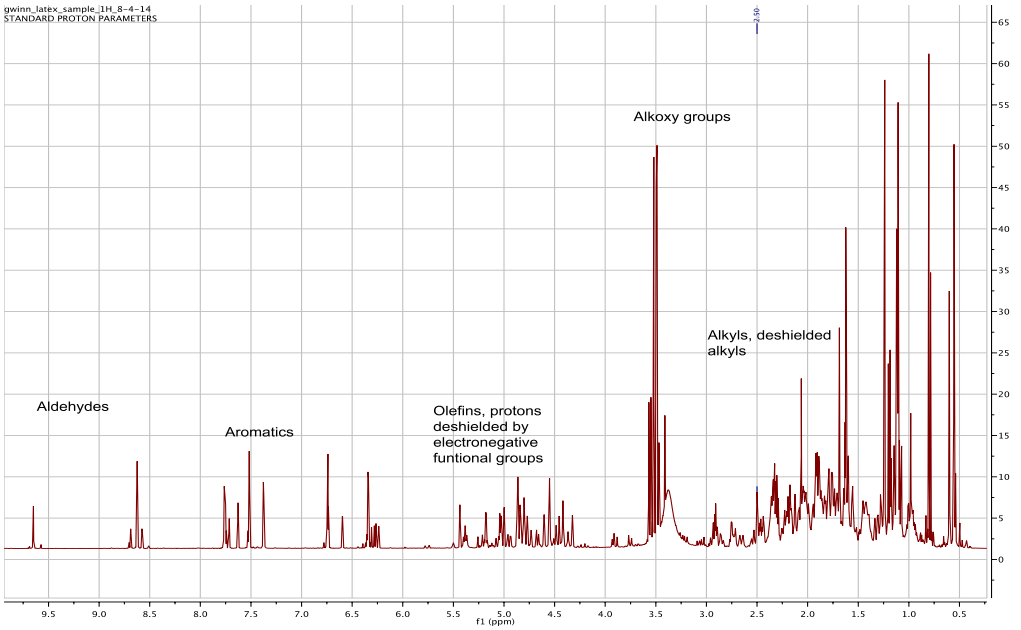

Figure 17. ^{1}H Nuclear magnetic resonance (NMR) spectrum of lyophilized *S. verticillata* resin.

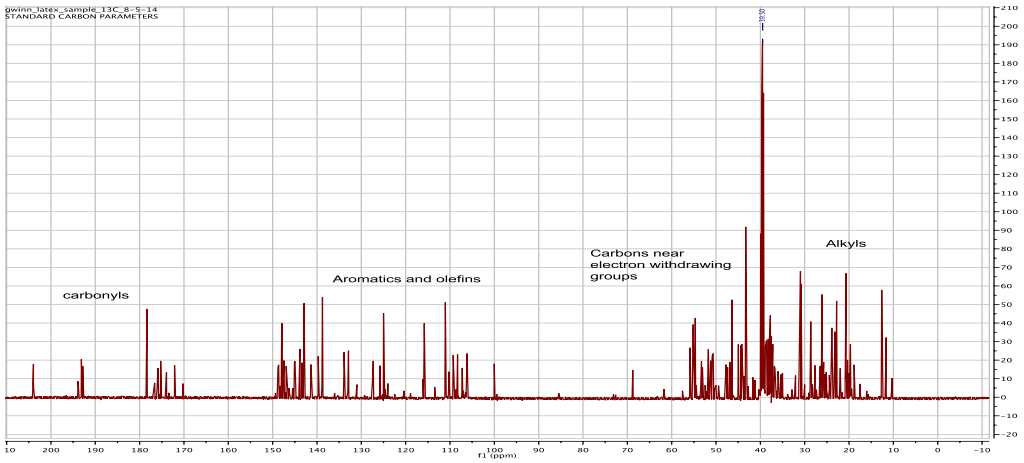

Figure 18. ^{13}C Nuclear magnetic resonance (NMR) spectrum of lyophilized *S. verticillata* resin.

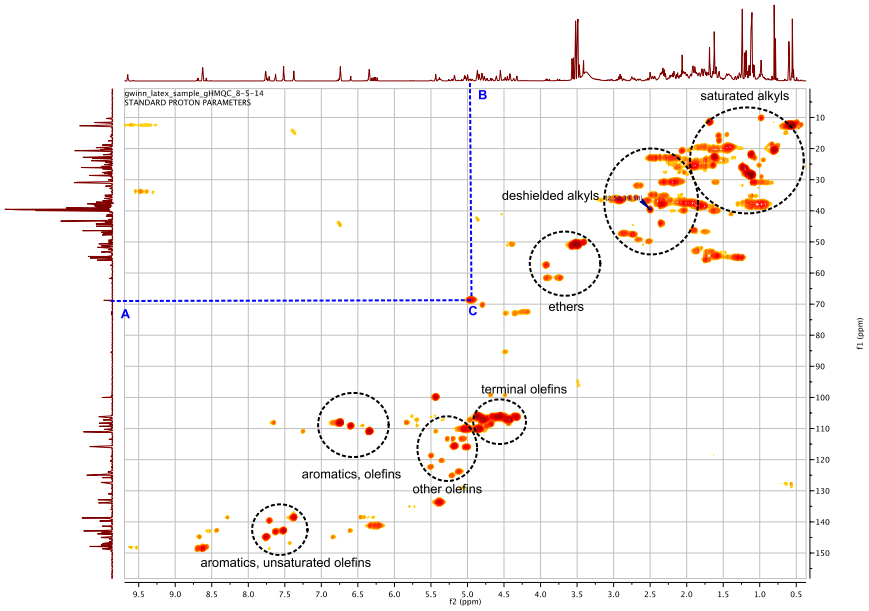

Figure 19. HMQC spectrum of lyophilized resin sample with correlated C and H.

NMR detected signals consistent with aldehydes, organic compounds containing –CHO functional group (McNaught *et al*., 2006). Chemical reactivity and biological function of aldehydes molecular size, with smaller aldehydes, such as formaldehyde and acetaldehyde being completely soluble in water (McNaught *et al*., 2006).Most sugars are derivatives of aldehydes and it is expected that the resin would contain aldehyde-derived sugars that could serve as a potential carbon source for bacteria and fungi **(**Langenheim, 2003; Kohlpaintner *et al*., 2008). Because of high reactivity of the formyl group, aldehydes are potential antimicrobials and possibly one of the classes of compounds in *S. verticillata* resin causing antimicrobial effect reported earlier in this research. (McNaught *et al*., 2006). Volatile aldehydes range from pungent odors to more favorable odors (Perfume #5 from CHANEL™) with traces of many aldehydes found in essential oils (e.g., cinnamaldehyde, and vanillin) (Kohlpaintner *et al*., 2008; McNaught

et al., 2006). Aldehydes degrade in air through autoxidation tending to oligomerize or polymerize and is the principal precursor to 2-ethylhexanol, which is used as a plasticizer (Kohlpaintner *et al*., 2008). This ability to polymerize could be a contributing factor to *S. verticillata* resin ability to quickly harden when exposed to the atmosphere.

NMR also detected signals consistent with aromatic hydrocarbons (arenes or aryl hydrocarbons), a hydrocarbon with sigma bonds and delocalized pi electrons between carbon atoms forming rings (Larson, 2002). The configuration of six carbon atoms in aromatic compounds is known as a benzene ring and is commonly used to make some types of rubbers, lubricants, dyes, detergents, drugs, explosives, and pesticides (Larsson *et al*., 1983; Larson, 2002). Aromatic hydrocarbons can be monocyclic (MAH) or polycyclic (PAH) (Larson, 2002). Naphthalene is the simplest example of a PAH and is found in oil, coal, and tar deposits, and are produced as byproducts fuel burning (Larson, 2002). Aromatic hydrocarbons were expected to be resin components, due to the obvious pine-like odor of the resin and previous research on conifer resins (Langenheim, 2003). Aromatic hydrocarbons could possibly be contributors to the antimicrobial activity reported earlier and also serve as a carbon source in the probiotic activity reported. Many aromatic hydrocarbons, such as terpenes, are high-value chemicals in the food, cosmetic, pharmaceutical, and biotechnology industries (Augustin *et al*., 2015; Thimmappa *et al*., 2015). Even though chemical synthesis of aromatics is problematic because of their complex structure, and with plants producing very small amounts of these valuable chemicals, making it difficult, time consuming and expensive to extract them directly from plants, *S. verticillata* resin may still be a potential source for both known and yet unknown aromatic compounds (Thimmappa *et al*., 2015).

NMR detected signals consistent with unsaturated hydrocarbons that contain at least one carbon–carbon double bond (alkenes), commonly known as olefins (Wade *et al*., 2006). The words alkene, olefin, and olefine are used interchangeably (Wade *et al*., 2006). Alkenes have two hydrogen atoms less than the corresponding alkane (with the same number of carbon atoms), an example being the simplest alkene, ethylene (C_2H_4) (Wade *et al*., 2006). Aromatic compounds are often drawn as cyclic alkenes, but their structure and properties are different and they are not considered to be alkenes (Wade *et al*., 2006).Olefins are colorless, nonpolar, combustible, and almost odorless, with the physical state depending on molecular mass (Wade *et al*., 2006). Ethene, propene, and butene are gases at room temperature, linear alkenes of five to sixteen carbons are liquids, and higher alkenes are waxy solids (Wade *et al*., 2006**)**.Alkenes are used in the petrochemical industry because they can participate in a wide variety of reactions, including polymerization and alkylation (Rodriguez-Corres *et al*., 2012).Polymerization of alkenes yields polymers of high industrial value, such as the plastics polyethylene and polypropylene (Rodriguez-Corres *et al*., 2012).

Olefins are present in other conifer species resin, notably the pines, so the presence of olefins in *S. verticillata* resin is not unexpected (Rodriguez-Corres *et al*., 2012). Olefins could be contributing to antimicrobial activity due to their high reactivity and their ability to bind to other molecules by breaking a double or triple bonds, but could also be serving as a carbon source for bacteria and fungi. Olefins may be responsible for *S. verticillata* resin polymerizing to its waxy form, once the volatiles have escaped.

NMR detected signals consistent with alkyls, an alkane missing one hydrogen (C_nH_{2n+1}) and are typically part of a larger molecule (Mallavadhani *et al*., 2013). Alkylation is an operation

in refineries used in the production of high-octane gasoline and alkylating antineoplastic agents are used to treat cancer. In medicinal chemistry, the incorporation of alkyl chains into some chemical compounds increases their lipophilicity and has been used to increase the antimicrobial activity of flavanones and chalcones (Mallavadhani *et al*., 2013).The presence of alkyls is *S. verticillata* resin was not unexpected because alkyls are a component of many larger organic functional groups/molecules such as alkoxy groups. Alkyls may be responsible for the resin's lipophilicity and thus its ability to cross the membranes of bacteria, either causing or carrying with it the cause of the antibacterial activity reported earlier. This ability to cross membranes could have additional applications for the resin in cancer research and drug delivery systems.

NMR detected signals consistent with alkoxy groups, an alkyl group bonded to oxygen (R–O). If bonded to hydrogen, alkoxy groups are alcohols and could be contributors to the antimicrobial effect.

NMR also detected signals consistent with carbonyls, a functional group composed of a carbon double-bonded to an oxygen atom (C=O). It is common to several classes of organic compounds, as part of many larger functional groups. Carbonyl groups are found in many antimicrobial compounds such as ketones, aldehydes, and carboxylic acids, which could be contributing to the antimicrobial activity of the resin.

NMR techniques have confirmed that *S. verticillata* resin is a complex mixture of both volatile and non-volatile components, many of which are antimicrobial and are used in medicinal chemistry. NMR has verified the presence of the chemical classes containing the earlier GC-MS detected volatiles such as the pinenes.

FTIR. Peaks and peak ratios in the LN tree were consistent with the previous reports (Tappert *et al*., 2011) (Figures 20 and 21). There was a broad peak at 3400 cm^{-1} which is attributed to the symmetrical stretching of O-H bonds. There was a small peak at 3076 cm^{-1} that Tappert *et a*l. (2010) attributed to C-H stretching of monoalkyl groups. There were several peaks in the area of aliphatic single C-H bonds, a very strong peak at 2933 cm^{-1}, and a small shoulder at 2960 cm^{-1}, as well as peaks at 2872 and 2848 cm^{-1}. The peak at 2848 cm^{-1} was strong which is typical of cupressaceous resins (Tappert *et al*., 2011). There was a strong peak at 1683 cm^{-1} that overlaps with one at 1721 cm^{-1}; these were related to C=O in carboxyl groups of resin acids. A medium intensity peak was located at 1640 cm^{-1}, which can be attributed to an O-H bending band (Tappert *et al*., 2011). As in the previous report the spectral range between 1550 and 650 cm^{-1} contained the largest number of peaks. There was a distinct peak at 1448 cm^{-1}, as is typical of cupressaceous resins, and of course the distinctive Baltic shoulder region at 1180 cm^{-1} (Tappert *et al*., 2011).

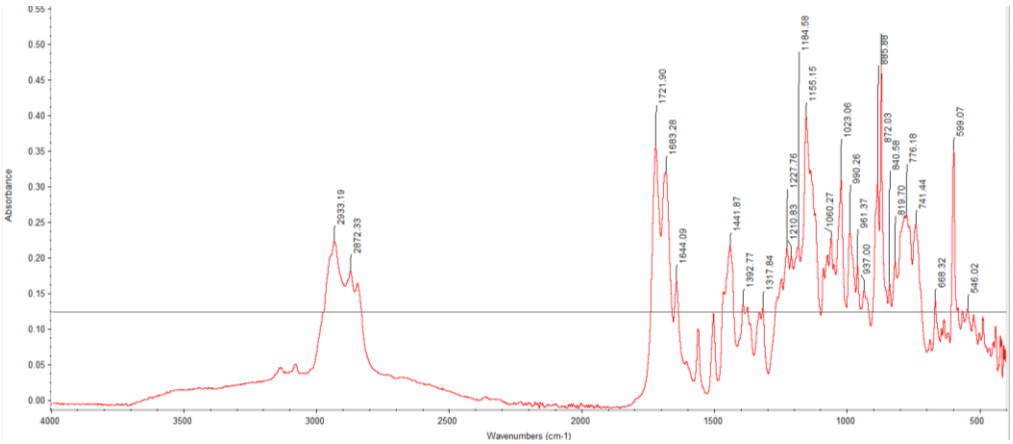

Figure 20. FTIR spectrum of lyophilized resin from *Sciadopitys verticillata*. Area depicted shows peaks in spectra between 400-4000 wavenumber (cm^{-1}).

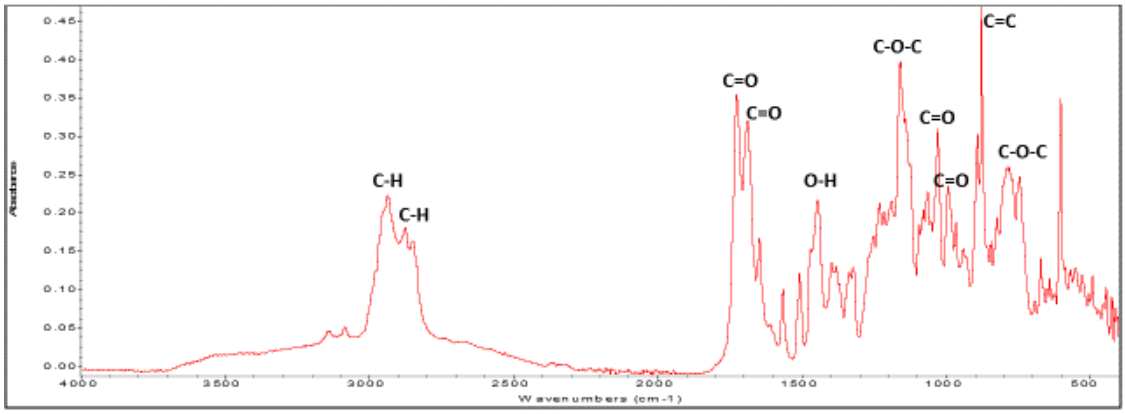

Figure 21. FTIR spectrum of lyophilized resin from *Sciadopitys verticillata* with major peaks identified.

Functional groups identified from the FTIR spectra are consistent with the NMR data. The functional groups associated with the identified NMR chemical classes were all present as major peaks in the FTIR spectra. Peak positions and intensities were similar to well-studied FTIR peaks associated with sugars (Xu *et al*., 2013) (Table 3). Possible polysaccharides present in the resin are cellulose and hemicellulose that are major constituents of plant cell walls, suitable carbon sources for bacteria and fungi, and a useful fuel source (Example: cellulosic alcohol) (Xu *et al*., 2013). The distinct peaks associated with lignin were also present in the resin samples (Xu *et al*., 2013). Lignins are crosslinked phenolic polymers and are second only to cellulose in abundance among natural polymers on earth (Xu *et al*., 2013). Lignins are not only used for cell wall structure, but have been identified as playing a role in conducting water in plant stems due to lignin's hydrophobicity.

When comparing LN fresh, lyophilized, and autoclaved resin, no obvious differences were visually detected between spectral peaks in the 500-3000 cm^{-1} range. There are obvious

differences in the spectras above 3000 cm^{-1}, in the region usually associated with O-H stretching of water in the samples. Spectra peak height and intensities indicated fresh resin had more water than autoclaved and lyophilized resin, with lyophilized having the least amount of water. To verify the visual inspection and interpretation of the spectas, a principle component analysis was conducted comparing lyophilized and autoclaved resin to fresh resin spectra. There was a lack of distinct groupings in the PCA scatter plot comparing fresh to autoclaved resin, indicating that there is no differences in the resins (Figure 23).

PCA of the FTIR scores data from fresh and lyophilized resin indicated distinct sample group separation based on resin treatment. Approximately 97% of variance could be explained by PC1 (Figure 24).

Table 3. *Sciadopitys verticillata* resin FTIR major peak list. Table lists wavenumber (cm^{-1}) position and absorbance intensity of the ten largest peaks of interest. Functional groups tentatively assigned to the peak position are listed.

***Sciadopitys verticillata* Resin FTIR Major Peak List**

Position	Intensity	Functional Group	Possible Compound
872.03	0.470	C-O-C	Hemicellulose
885.88	0.303	C=C	Alkenyl
990.26	0.234	C=O	Cellulose
1023.06	0.309	C=O	Cellulose
1155.15	0.398	C-O-C	Cellulose
1441.87	0.216	O-H	Cellulose, hemicellulose, lignin
1683.28	0.320	C=O	Lignin
1721.90	0.354	C=O	Ketone, aldehyde
2872.33	0.180	C-H	Alkyl
2933.19	0.222	C-H	Lignin

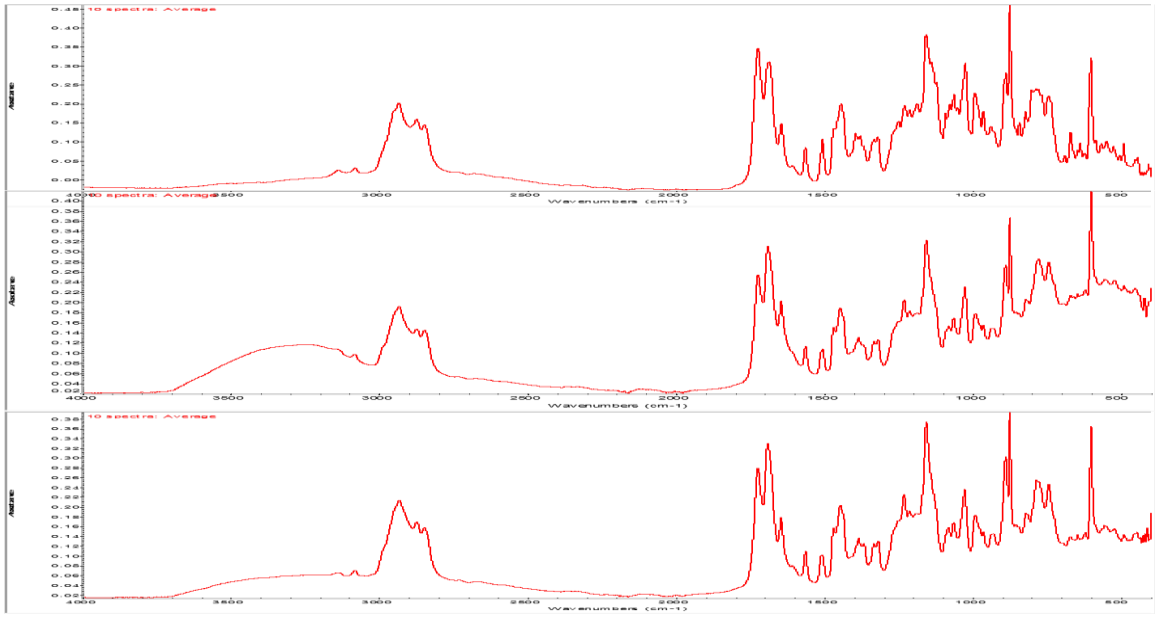

Figure 22. FTIR spectra of lyophilized, fresh, and autoclaved *Sciadopitys verticillata* resin. Averaged (10 replicates each) spectra of lyophilized (Top), fresh (Middle), and autoclaved (Bottom) resin samples alligned with major peaks, allowing for visual comparison of peak locations and intensity.

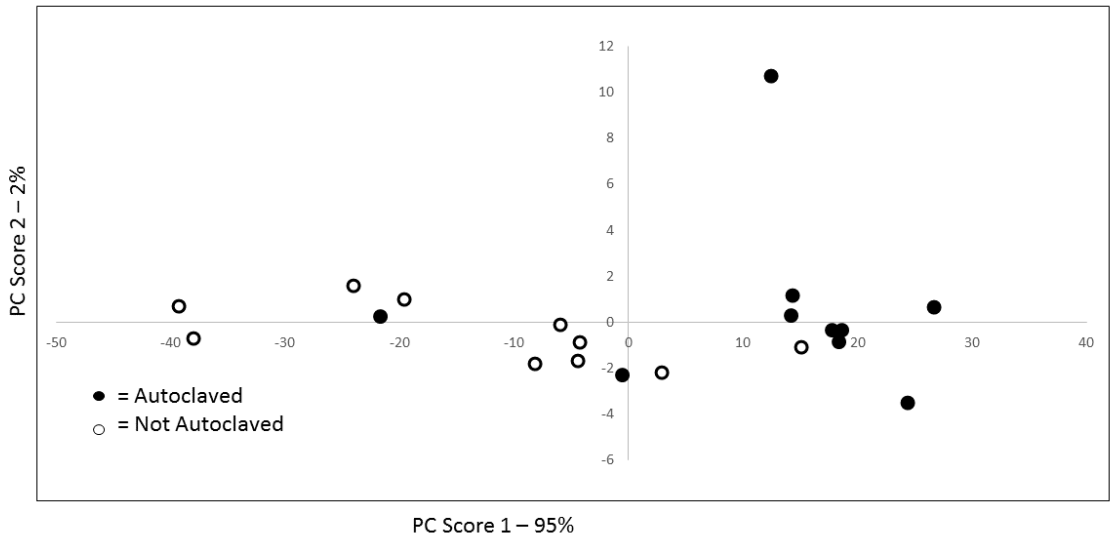

Figure 23. Principle component analysis scatter plot of FTIR spectra of freshly collected unautoclaved and autoclaved *Sciadopitys verticillata* resin. Lack of distinct sample groupings in respect to principle component 1, indicated that autoclaved and fresh unautoclaved samples were not significantly different.

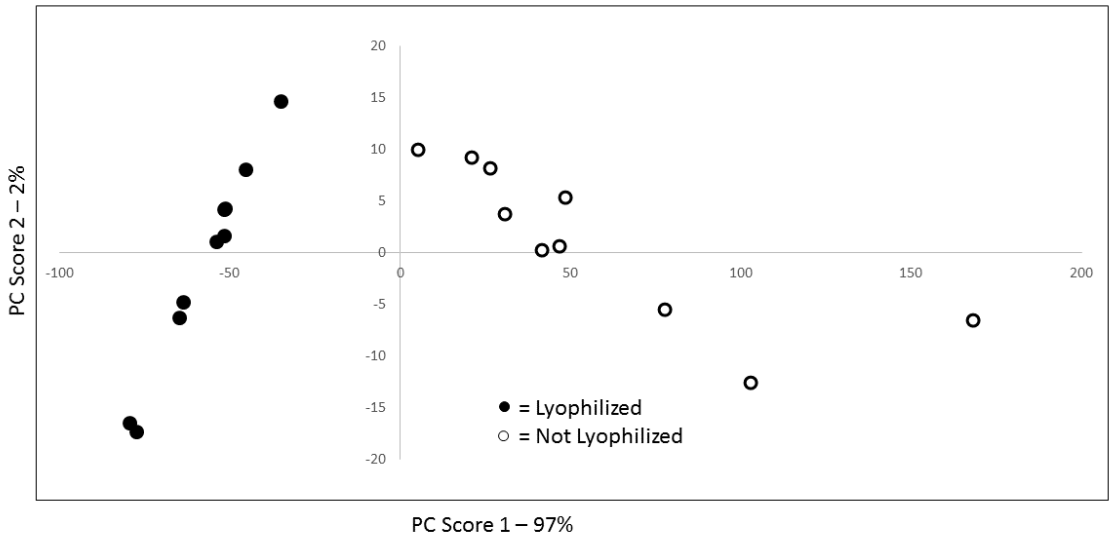

Figure 24. Principle component analysis scatter plot of FTIR spectra of *Sciadopitys verticillata* resin freshly collected and lyophilized. Scores plot of the first two PCs obtained by PCA of the mid-infrared spectra measured on the resins that were lyophilized or not lyophilized. Scatter plot did form distinct sample groupings, indicating that samples are different and that 97% of the variance can be explained by principle component 1.

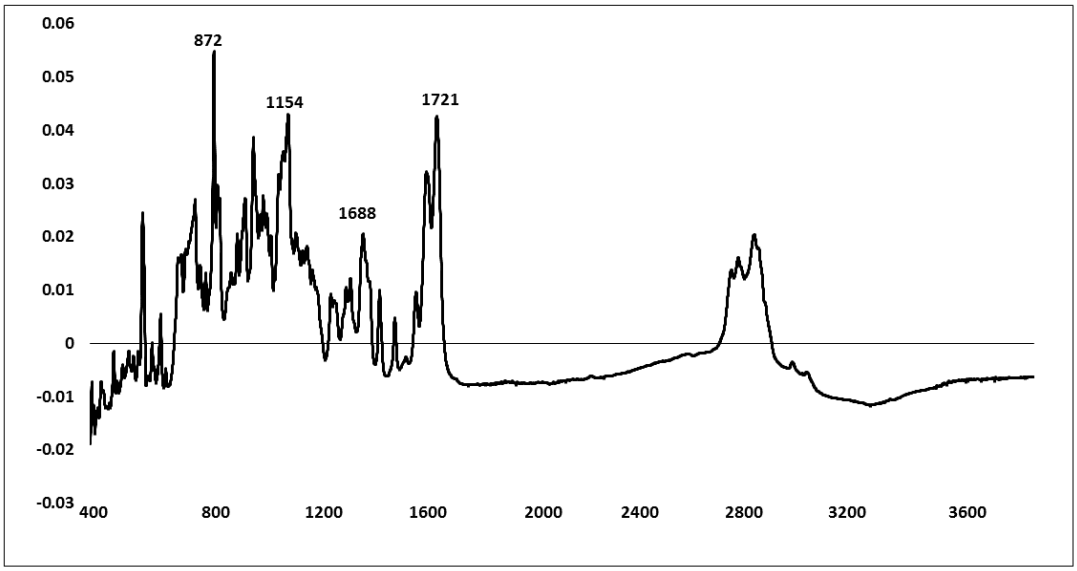

Figure 25. Loadings plot of the first principle component (See Figure 24) from FTIR spectra of *Sciadopitys verticillata* resin. Loadings was used to identify functional groups responsible for variance between the lyophilized and nonlyophilized samples.

FTIR analysis was successfully used to identify important functional groups present in the resin and link them to the chemical classes identified by NMR. This research also used FTIR to identify important carbohydrates such as cellulose and lignin in the resin. Based on PCA analysis it was determined that lyophilized, autoclaved, and fresh resin are the same in compositional components, but relative amounts of the components may be changing due to evaporation in the lyophilizing and autoclaving processes.

Table 4. Functional groups responsible for variance between freshly collected and lyophilized resin realized with respect to principle component 1. The top five peaks in the loadings graph were used to identify wavelength (Variable) responsible for variance with respect to principle component 1.

Loadings Five Highest Peaks
(Fresh vs Lyophilized)

Position	Functional Group
1721	C=O
1688	C=O
1154	C-O-C
872	C-O-C

Pyrolysis gas chromatography mass spectrometry. Peaks representing individual pyrolysis degradation products were identified and compared to the spectral library for tentative identification (Figure 26). Abundance was greater than 1% for eight pyrolysis products (Table 5), and these represented 38% of the total.

Pyrolysis products were separated into two distinct groups based on structure. One group was structurally related to communal (six pyrolysis products), a compound found in the Baltic

amber (Wolfe *et al*, 2009), and the other was likely derived from carotenoids (two pyrolysis products).

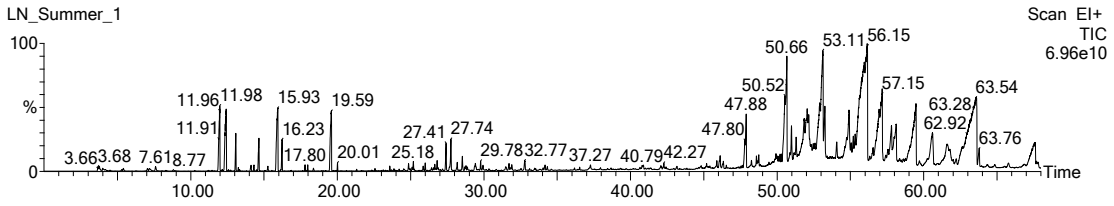

Figure 26. Pyrolysis GCMS pyrogram of resin from LN *Sciadopitys verticillata* tree.

Products related to communic acid are shown in Figure 27. This group shares distinct similarities in structure to communol (Figure 28). Pyrolysis products of Baltic amber contained communol-derived polymers with succinyl esters that crosslinked communol moieties (Poulin *et al*., 2012). Several of the pyrolysis products found in abundance in the resin of *S. verticillata* were also structurally related to communic acid and communol, components that are also part of the ether-insoluble fractions of Baltic amber (Wolfe *et al*., 2009) (Figure 28). Hexane extracts of *S. verticillata* seed contained large quantities of communic acid (Hasegawa *et al*., 1985). Communic acid is antibacterial and antifungal, and presence of it or closely related compounds provides further insights into the antimicrobial activity of the resin.

The primary pyrolysis product of the *S. verticillata* resin is the steroid, 3-ethyl-3-hydroxy-(5à)-androstan-17-one ($C_{21}H_{34}O_2$) (Figure 27-A), which comprised 13% of the total peak area. In a study on the insecticidal compounds in mango ginger (*Curcuma amada*), 3-ethyl-3-hydroxy-(5à)-androstan-17-one was the primary peak (94% of peak area) (Jegajeevanram *et*

al., 2014). In addition to insecticidal activity, 3-ethyl-3-hydroxy-(5à)-androstan-17-one had antibacterial, anticancer, anti-inflammatory, antiasthma, diuretic, antiarthritic, and insecticidal activities (Jegajeevanram *et al*., 2014). With this compound being the most abundant compound identified in the resin using Pyro-GCMS, it is likely that it or the compounds from which it was derived are major contributor(s) to the antimicrobial activity of the resin collected from S. *verticillata*.

The next two most abundant pyrolysis products are structurally similar to 27-A, and they represented a total of 11% of the peak area. The second most prevalent pyrolysis product (6 % of peak area), 3,12-bis(acetyloxy)-7-oxo-methyl ester (3à,5á,12à)-cholan-24-oic acid ($C_{26}H_{44}O_4$) (Figure 27-B), differs from 27-A in that it has an additional carbons (five) and a hydroxyl group. This compound can act as a detergent that aids in solubilizing fats for absorption and is commonly found in bile acid (Takemura *et al*., 2011) and is an inhibitor of reductase activity in *Escherichia coli* (Takemura *et al*., 2011).The third most abundant pyrolysis product was the steroid pregnenolone acetate 10,13-dimethyl-2-oxo-2,3,4,7,8,9,10,11,12,13,14,15,16,17-tetradecahydro-1H-cyclopental-acetic acid ($C_{23}H_{30}O_3$) (Figure 27-C) which is similar in structure to the two previously discussed products.

The most obvious difference between the most abundant compound (27-A) and 27-C is replacement of a hydroxyl group with a carbonyl group. Pregnenolone acetate is a precursor to other hormones that effect levels of progesterone and estrogen in the humans when taken orally (Al-Masoudi *et al*., 2015). Pregnenolone acetate is a common ingredient of anti-aging remedies because it works as a water-binding agent when applied to the skin, easily forming hydrogen bonds and hydrophobic interactions with amino acid residues (Al-Masoudi *et al*., 2015).

Table 5. Pyrolysis GCMS peaks greater than 1%.

Pyrolysis GCMS Peaks Greater >1% Total Peak Area			
RT	**Tentative Library ID**	**m/z and (Relative Intensities)**	**Average Peak Area %**
50.659	Methyl 3á-acetoxy-24,23-dinor-5á-chol-5-enoate	79 (52), 81 (91), 94 (52), 105 (89), 119 (53), 147 (68), 161 (100), 173 (83), 254 (60), 255 (62)	3
50.974	Retinoic acid methyl ester	81 (58), 91 (37), 95 (40), 105 (28), 119 (38), 131 (27), 145 (36), 173 (100), 255 (36), 314 (30)	1
51.839	(1S,5S,8aS)-5-[2-(3-Furyl)ethyl]-1,4a-dimethyl-6-methylenedecahydro-1-naphthalenecarboxylic acid	79 (38), 81 (100), 82 (43), 93 (22), 95 (40), 107 (28), 121 (41), 133 (30), 148 (24), 189 (28)	2
52.890	4a,5,6,7,8,8a-hexahydro-6-[1-(hydroxymethyl) ethenyl]-4,8a-dimethyl- 2(1H)-Naphthalenone	67 (22), 79 (36), 91 (28), 95 (100), 107 (29), 121 (95), 159 (46), 174 (52), 175 (58), 234 (49)	3
53.115	9-cis-Retinal	79 (52), 91 (48), 95 (52), 105 (44), 119 (48), 121 (100), 159 (59), 174 (68), 234 (50), 235 (27)	5
57.121	10,13-dimethyl-2-oxo-2,3,4,7,8,9,10,11,12,13,14,15,16,17-tetradecahydro-1H-cyclopental-Acetic acid	41 (22), 77 (41), 81 (100), 82 (76), 94 (88), 95 (57), 107 (32), 159 (80), 160 (41), 187 (28)	5
59.467	3,12-bis(acetyloxy)-7-oxo-methyl ester (3à,5á,12à)-Cholan-24-oic acid	43 (46), 91 (38), 95 (91), 105 (30), 119 (29), 159 (100), 172 (58), 173 (71), 251 (72), 311 (37)	6
63.569	3-ethyl-3-hydroxy-(5à)-Androstan-17-one	79 (59), 91 (72), 94 (100), 95 (70, 105 (63), 145 (44), 160 (79), 161 (52), 173 (50), 175 (28)	13

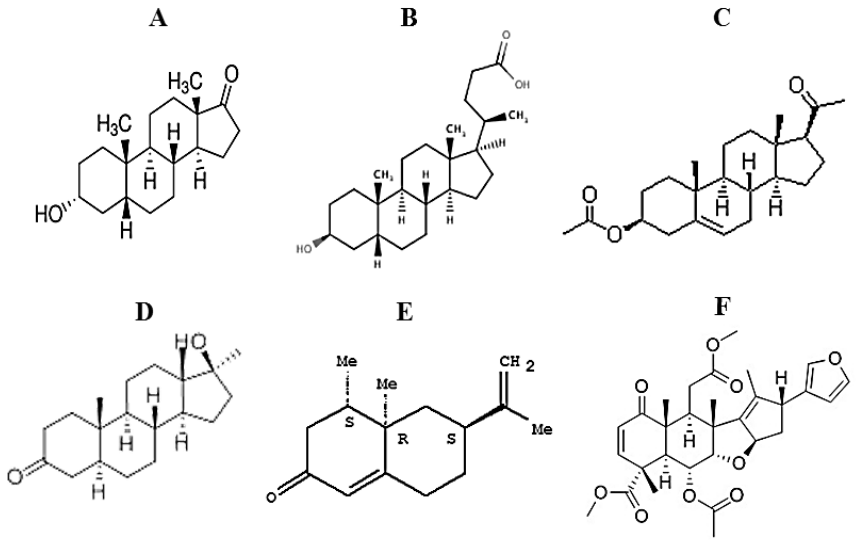

Figure 27. Pyrolysis products from *Sciadopitys verticillata*. Six of the eight major resin pyrolysis products proposed are 3-ethyl-3-hydroxy-(5à)-Androstan-17-one (A), 3,12-bis(acetyloxy)-7-oxo-methyl ester (3à,5á,12à)-Cholan-24-oic acid (B), 10,13-dimethyl-2-oxo-2,3,4,7,8,9,10,11,12,13,14,15,16,17-tetradecahydro-1H-cyclopental-Acetic acid (C), 1S,5S,8aS)-5-[2-(3-Furyl)ethyl]-1,4a-dimethyl-6-methylenedecahydro-1-naphthalenecarboxylic acid (D),4a,5,6,7,8,8a-hexahydro-6-[1-(hydroxymethyl) ethenyl]-4,8a-dimethyl-, 2(1H)-Naphthalenone (E), and Methyl 3á-acetoxy-24,23-dinor-5á-chol-5-enoate (F).Structures shown are from Chemsynthesis.com.

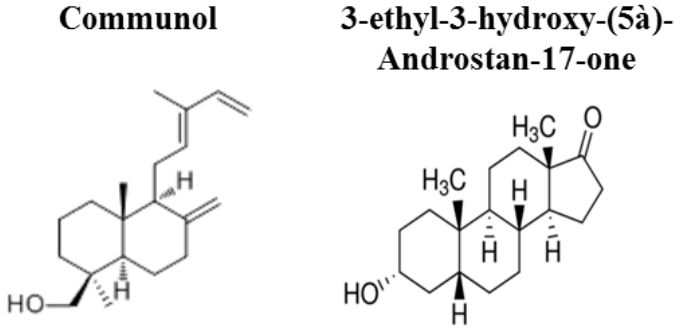

Figure 28. Comparison of communal and 3-ethyl-3-hydroxy-(5à)-androstan-17-one. Distinct similarities are evident when structures are comparing the major pyrolysis products to communol. Structures shown are from Chemsynthesis.com.

Pregnenolone acetate inhibited hydroxylase enzymes in *E. coli*, possibly making the bacteria less fit for survival due to lower availability of food (Al-Masoudi *et al*., 2015).

Together, the next three most prevalent pyrolysis products related to communal comprise only 8% of the total peak area. The compound (1S,5S,8aS)-5-[2-(3-furyl)ethyl]-1,4a-dimethyl-6-methylenedecahydro-1-naphthalenecarboxylic acid ($C_{20}H_{32}O_2$) represented 2% of the total peak area (Figure 27-D), and it is similar in structure the 27-A. It has one fewer carbon and two fewer hydrogens, and the ester in 27-A is replaced by a hydroxyl group. Pure 27-D is a white to off-white crystalline powder that is used as an anabolic steroid and is classified as a hydroxyketosteroid (Ndukwe *et al*., 2007).The proposed pyrolysis product, 4a,5,6,7,8,8a-hexahydro-6-[1-(hydroxymethyl) ethenyl]-4,8a-dimethyl-,2(1H)-naphthalenone ($C_{15}H_{22}O_{2)}$ is possibly a degradation product of the other compounds shown in Figure 27. 27-E has been isolated from *Kirganelia reticulata* a member of the resin producing Euphorbiaceae family that includes *Hevea brasiliensis*, the rubber tree (Sudha *et al*., 2013).

Approximately 3% of the total peak area was due to nimbin, methyl 3á-acetoxy-24,23-dinor-5á-chol-5-enoate ($C_{30}H_{36}O_9$) (Figure 27-F) Nimbin is a bitter-tasting, pale yellow solid limonoid (Roy *et al*., 2006). Compounds belonging to the highly oxygenated limonoid group have reported insecticidal, insect antifeedant and growth regulating activity on insects, antibacterial, antifungal, antimalarial, anticancer, and antiviral activity (Roy *et al*., 2006; Jacob *et al*., 2000). Hundreds of modified terpenoid limonoids have been isolated from various plants, but only studies of its isolation from plant families of the order Rutales have been reported (Roy *et al*., 2006; Jacob *et al*., 2000). Meliaceae (Mahogany) and Rutaceae (Citrus) families contain the highest levels of limonoids, and lower levels are found in Cneoraceae and Simaroubaceae

families (Roy *et al*., 2006). Even though it is only a small portion of the pyrolysis products, 27-F may have contributed biological activity of the resin. With the abundance of oxygen on the periphery of the compound, there is a possibility of reactive oxygen species being formed that could be contributing to this antibacterial activity. If confirmed, this would be a rare report of limonoids outside the earlier mentioned plant families.

The six pyrolysis products in Figure 27 total approximately 35% of the total peak area. It is probable that 27-F, being the more complex structure of the group, is either the parent compound of the other five pyrolysis products or along with the other five is a component of a larger yet unidentified compound. With the antimicrobial activity and ability to form reactive oxygen species and hydrogen bonds of members of this group, it is possible that the antimicrobial activity of the pinenes tested earlier is enhanced by this group and this could account for the difference in the antibiotic activity between *S. verticillata* resin and the pinenes.

The second group of structurally similar pyrolysis products proposed are likely pyrolysis products of plant carotenoids (Auldridge *et al*., 2006). Retinoic acid methyl ester (A) ($C_{21}H_{30}O_2$) and 9-cis-retinal (B) ($C_{20}H_{28}O$) (Figure 29) comprise 1% and 5% total peak areas respectively. These compounds are forms of Vitamin A and known to be inducers of cell differentiation that have been formulated into treatments for acne, hyper- and hypo-pigmentation, psoriasis, the reduction of wrinkling of the skin as an incident of aging, and promoting the rate of wound healing, and limiting of scar tissue formation during healing (Panzella *et al*., 2004).Vitamin A is a group of unsaturated nutritional organic compounds that includes retinol, retinal, retinoic acid, and carotenoids, such as beta-carotene (Panzella *et al*., 2004). Retinal, retinol and retinoic acid

are the aldehyde, alcohol and acid forms of vitamin A and exist as many geometric isomers due to the unsaturated bonds in the aliphatic chain.

These retinoids have no reported antimicrobial activity and combined, make up only 6% of the total peak area and therefore are probably not causing the antimicrobial activity of the resin. However, with several unsaturated areas these compounds are potentially reactive, being able to attach to other compounds making them inactive.

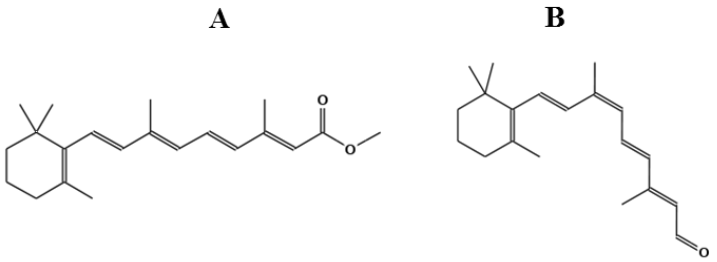

Figure 29. Retinoic acid methyl ester (A) and **9-cis-retinal (B).**Retinoic acid methyl ester and 9-cis-retinal structures are similar. Structures shown are from Panzella *et al*., 2004.

Comparison of resin source trees by pyro-GCMS. Comparison of the chemical complex of different sources of *S. verticillata* resin was investigated by pyro-GCMS. There were no detectable differences between the pyrograms collected from LN resin and those of resins collected from VA, WG, or UT (Figure 30). This apparent lack of differences was verified by PCA. (Appendix 6). Since UT and LN (trees with the greatest difference in elevation - 345 m) were not different, elevation does not appear to have a role in chemical changes in resin pyrolysis products. Mean monthly temperature and rainfall (variable that typically differ with

elevation) were different by 2 °C and 2 cm, respectively, at the UT and LN locations. Since the LN and FL trees were clones from the same plant material, it was unexpected that the pyrolysis products of resins collected from these trees should differ. The differences in the two pyrograms were primarily in the mid-range. In order to evaluate the impact of individual tree, PCA was employed, and PCA scores separated on PC1 except for one outlier from LN (Figure 31). The corresponding loadings plot of PC1 is displayed in Figure 31. The loadings plot reveals the degree of the contribution of chromatographic peak area percentage to the differences among the samples. Since the peaks are proportional to the relative contribution of a given peak area, the plot was used to identify pyrolysis products responsible for variance associated with PC1 (Figure 31) (Table 6). Presence of α-pinene was confirmed (Figure 32).

In comparisons of LN and FL, five compounds were primarily responsible for the variance in PC1, most of which were aromatics (Table 6) (Figure 31). Peak areas were greater in the LN resin for two compounds related to the terpines than in the FL pyrogram. The first of these two compounds, 1,3,5,5-tetramethyl-1,3-cyclohexadiene, is a naturally occurring derivative of the terpinene1,3-cyclohexadiene, a clear colorless to light yellow liquid component of pine oil (Figure 33-A) (Campbell *et al*., 2011). It was also the largest peak in the loadings plot. Another significant product was tentatively identified as the sesquiterpene, octahydro-7-methyl-3-methylene-4-(1-methylethyl)-1H-cyclopenta[1,3]cyclopropa[1,2]benzene($C_{15}H_{24}$), a stereoisomer of β-cubebene. β-cubebene has a citrus odor, and was earlier identified in this research as a *S. verticillata* resin component by GC-MS (Figure 33-C).

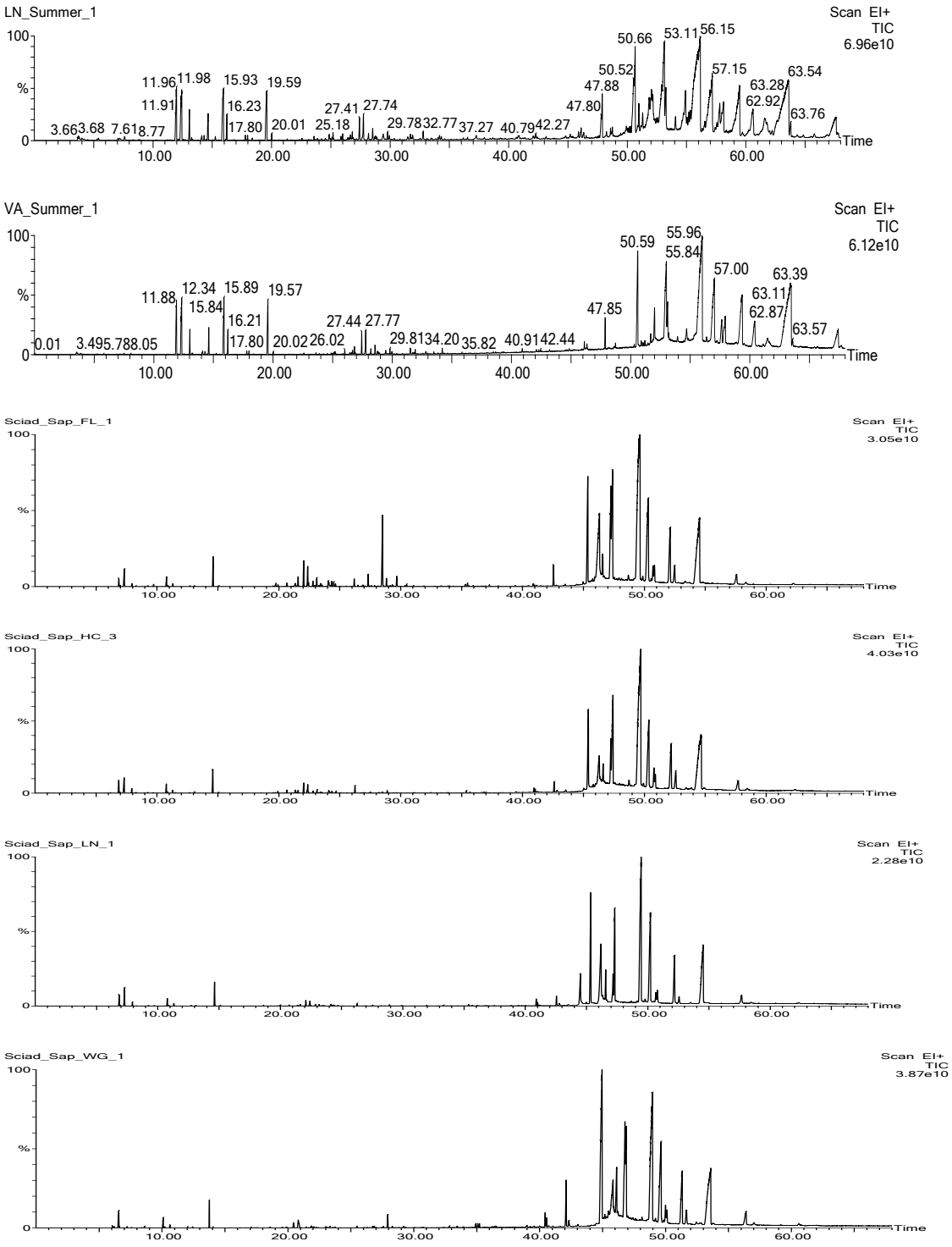

Figure 30. Pyrolysis GCMS pyrograms of resin from *Sciadopitys verticillata* trees used as resin sources. The LN and VA pyrograms shown were analyzed at lower thresholds than the other resin sources and show more peaks than the other samples

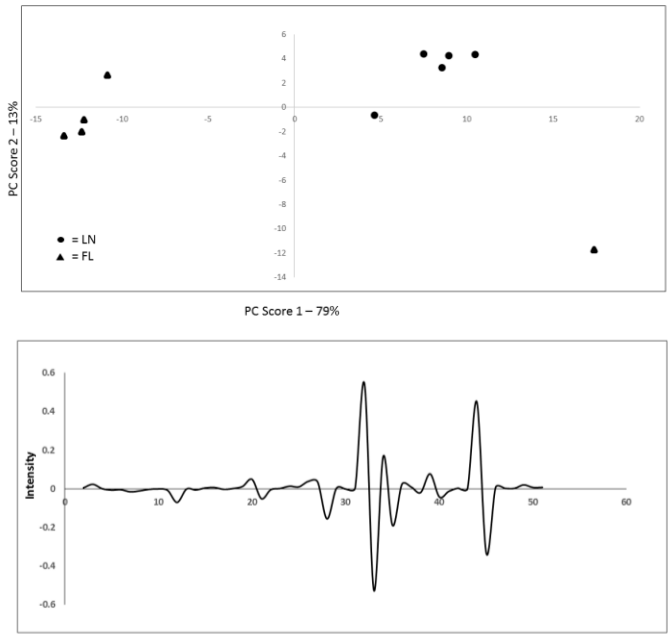

Figure 31. PCA scatter plot and loadings plot of LN *vs* FL. Pyro-GCMS PCA score plots for comparison of LN and FL resins. Samples separated into distinct groups with respect to PC1.

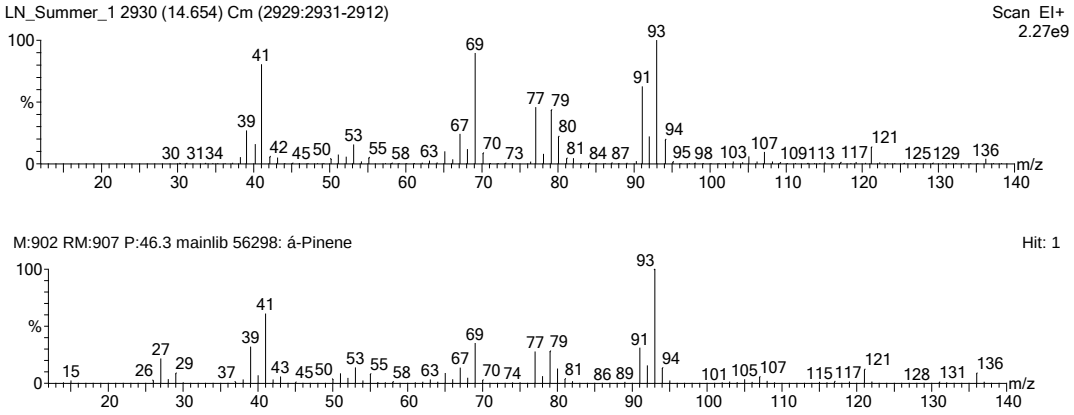

Figure 32. Pyrogram of pinene. Example of pyrograms used to identify compounds of interest from PCA loadings plot. Compounds identified from the PCA loadings were examined for tentative identification of the compound.

The remainder of the products identified in the loadings plots had greater peak areas in the FL resin. The second largest peak in the loadings graph was tentatively identified as 3-(2-propenyl)-cyclohexene ($C_{14}H_{18}O_4$) (Figure 33-B), that has a cycloalkene at its core (Campbell *et al*., 2011). Cyclohexenes are colorless, flammable liquids with distinctive detergent-like odor often used in detergents and for the industrial production of precursors to nylon (Campbell *et al*., 2011). The pyrolysis product tentatively identified as 1,2,3,4,4a,5,6,8a-octahydro-7-methyl-4-methylene-1-(1-methylethyl)-,1á,4áá,8áá)-naphthalene ($C_{15}H_{24}$) is a stereoisomer of γ-cadinene, identified earlier in this research by GC-MS (Figure 33-D).

The cadinenes are bicyclic sesquiterpenes that occur in many essential oil-producing plants (Borg-Karlson *et al*., 1981). The final product that was larger in the FL resin than in the LN was α-Pinene which, in a GC-MS analysis, was identified as the primary component of lyophilized *S. verticillata* resin. This compound is commonly found in the oils of many species of coniferous trees and is antimicrobial (Borg-Karlson *et al*., 1981).

Table 6. Tentatively identified compounds from LN *vs* FL loadings plot.

RT	Tentative ID	Resin With Largest Peak
14.656	α-Pinene	FL
20.011	1,3,5,5-Tetramethyl-1,3-Cyclohexadiene	LN
23.578	3-(2-propenyl)-Cyclohexene	FL
27.414	Octahydro-7-methyl-3-methylene-4-(1-methylethyl)-1H-cyclopenta[1,3]cyclopropa[1,2]benzene(common name β-cubebene)	LN
29.940	1,2,3,4,4a,5,6,8a-octahydro-7-methyl-4-methylene-1-(1-methylethyl)-,1á,4áá,8áá)-naphthalene (common name γ-cadinene)	FL

The pyrolysis products contributing to the differences between FL and LN were relatively low in abundance, equal to approximately 1% of total peak area of the pyrolysis GCMS pyrograms. With the exception of α-Pinene (Figure 33-E), none of the major antimicrobial pyrolysis products identified earlier were the principle components used for detecting variance between samples.

The LN and the FL were clones from the same parent plant and located within 1.5 km of one another, but one was in full sun (LN) whereas the other was in full shade (FL). The differences in the two pyrograms were not based on the potentially antimicrobial components of the resin that make up more than 1% peak area of the pyrolysis products. However, the volatile α-pinene was identified as responsible for variance in the pyrolysis products of the samples. This indicates that sunlight may have an influence on α-pinene production, but may not have much influence on production of the before mentioned antimicrobial components that make up the bulk of the resin.

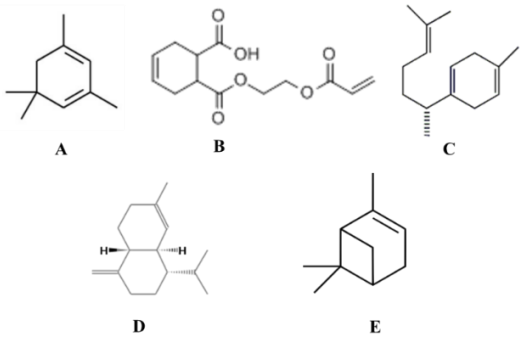

Figure 33. Structures of tentatively identified pyrolysis products from LN *vs* FL loadings plot. Five of the pyrolysis products tentatively identified were 1,3,5,5-Tetramethyl-1,3-Cyclohexadiene (A), 3-(2-propenyl)-Cyclohexene (B), octahydro-7-methyl-3-methylene-4-(1-methylethyl)-1H-cyclopenta[1,3]cyclopropa[1,2]benzene or β-cubebene (C),1,2,3,4,4a,5,6,8a-octahydro-7-methyl-4-methylene-1-(1-methylethyl)-,1á,4áá,8áá)-naphthalene or γ-cadinene (D), and α-pinene E. Structures shown are from Chemsynthesis.com (B and D) and ChemDraw (A, C and E).

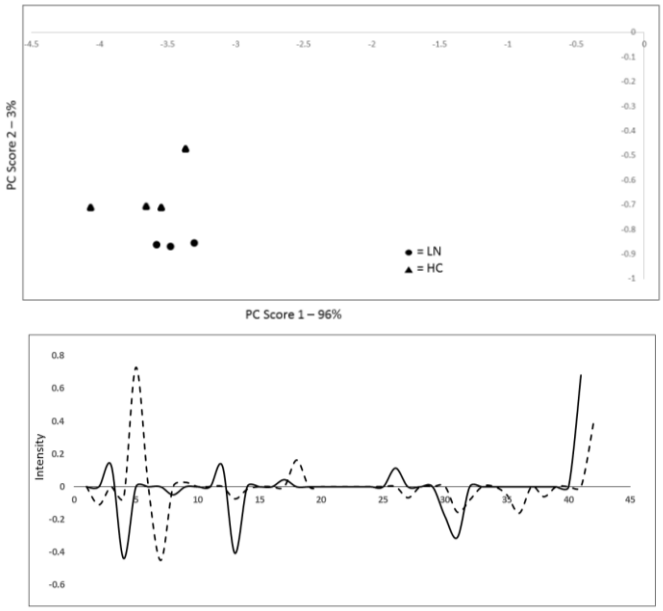

Figure 34. PCA scatter plot and loadings plot of LN *vs* HC. HC and LN separated into distinct groups on the scatter plot with respect to PC2, but not PC1.

The LN resin was also different from HC resin in the low to mid-range (3-20 minute retention) of the pyrograms. Observed differences were verified using PCA, and PCA scores for HC separated from LN on PC2 but not PC1 (Figure 34). Resin from HC differed from LN primarily in volatile monoterpene pyrolysis products (Table 7).

The pyrolysis product represented by the largest peak in the loadings graph was tentatively identified as carbon dioxide (CO_2) (Figure 35-A). Carbon dioxide was quickly (3.5 minutes RT) liberated in the pyrolysis process, probably from a larger compound, or was a resin component itself. Carbon dioxide is needed for photosynthesis and released during cellular respiration and it is not surprising that carbon dioxide is in the resin.

The HC tree is growing in partial shade and probably not photosynthesizing as much as the LN tree growing in full sun and therefore not producing as much CO_2.

Table 7. Tentatively identified compounds from LN *vs* HC loadings plot.

HC Pyro GCMS PCA Loadings Peaks Identified	
RT	**Tentative ID**
3.515	Carbon dioxide
7.606	Phenol
14.594	α-Pinene
20.011	1,3,5,5-Tetramethyl-1,3-Cyclohexadiene

The pyrolysis product represented by the second largest peak in the loadings graph was tentatively identified as phenol (C_6H_5OH) (Figure 35-B). Phenol, sometimes called carbolic acid, is a volatile aromatic white crystalline solid that consists of a phenyl group ($-C_6H_5$) bonded to a hydroxyl group (−OH). It is mildly acidic precursor to many materials and useful compounds (Kütt *et al.,* 2008). It is primarily used to synthesize plastics and related materials, such as polycarbonates, epoxies, Bakelite™, nylon, detergents, pharmaceutical drugs (notably aspirin). Phenol is widely used as an antiseptic (Hanscha *et al*., 2000).

Phenol's hydrophobic effect and the formation of phenoxyl radicals are its probable mechanism for toxicity to bacteria and may be a contributing factor to the antimicrobial effect of *S. verticillata* resin (Hanscha *et al*., 2000).

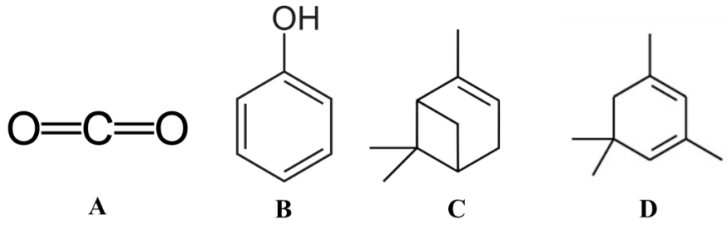

Figure 35. Structures of tentatively identified pyrolysis products from LN *vs* HC loadings plot. Four of the pyrolysis products tentatively identified were carbon dioxide (A), phenol (B), α-pinene(C), and 1,3,5,5-Tetramethyl-1,3-Cyclohexadiene (D).Structures shown are from ChemDraw.

Phenol's hydrophobic effect and the formation of phenoxyl radicals are its probable mechanism for toxicity to bacteria and may be a contributing factor to the antimicrobial effect of *S. verticillata* resin (Hanscha *et al*., 2000).The other two pyrolysis products represented by the PCA loadings graph were the previously discussed, α-Pinene and 1,3,5,5-Tetramethyl-1,3-Cyclohexadiene(Figure 35-C and 35 D).

The sites of these two trees differed slightly in elevation and in available sunlight, but had significant differences in monthly rainfall. This study provides an indication that environment may play a role in the chemistry of the resins, but true effects may be masked due to small sample size and lack of environmental control.

Differences in PCA of resin from different source trees were not different in the major pyrolysis products, but different in the volatiles. This indicates that it should not matter which tree is used for collecting resin for use as an antimicrobial or probiotic. The difference in the LN, FL, and HC resin may be a site difference (sun vs shade). This sun vs shade difference has been reported to also effect resin quantities produced by *S. verticillata*, possibly due to increased photosynthesis and photosynthetic dependent compounds (Yates *et al*., 2006).

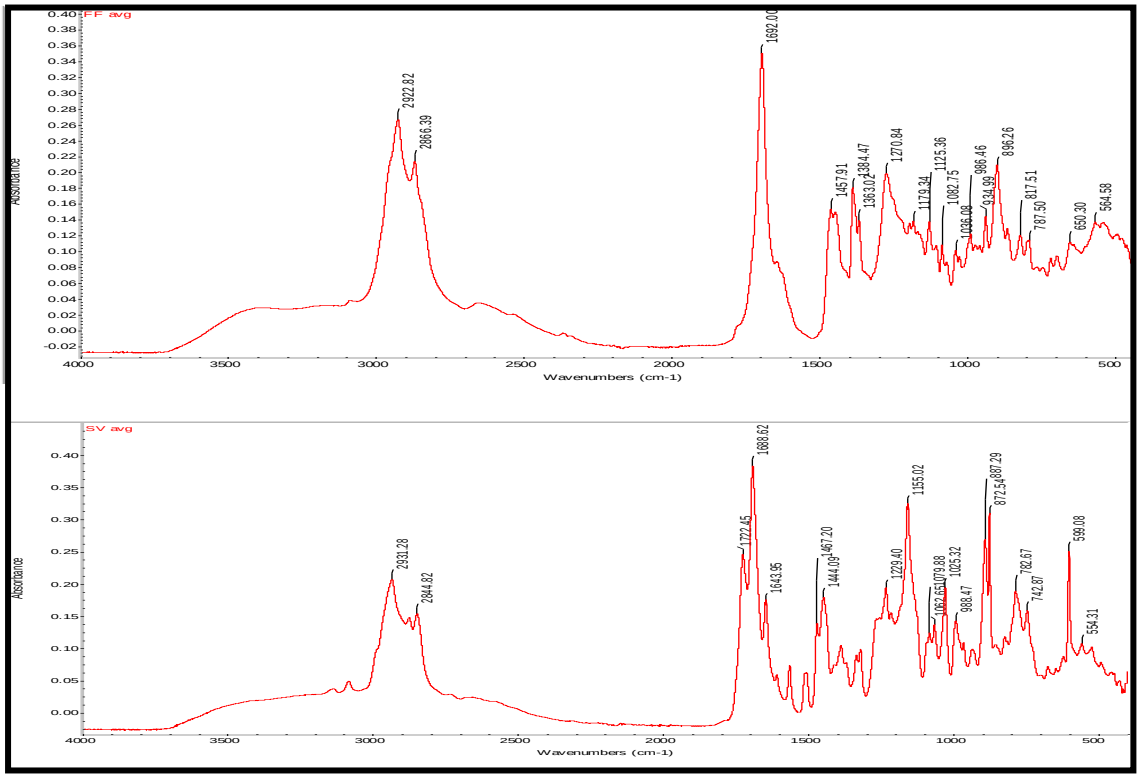

Figure 36. FTIR spectra of Fraser fir and *Sciadopitys verticillata* resin. FTIR spectra of Fraser fir (Top) and *S. verticillata* (LN) (Bottom) resin were visually compared for obvious differences in peak location and intensity

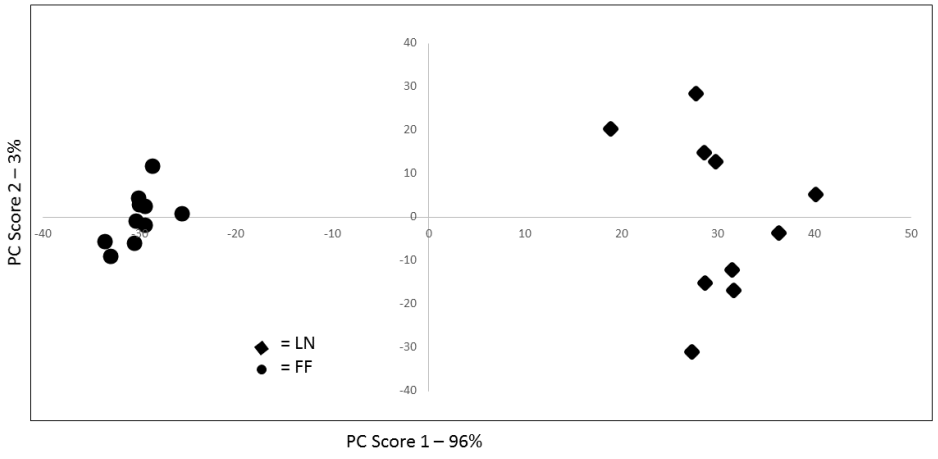

Figure 37. PCA of spectra of Fraser fir and *Sciadopitys verticillata* resin. Distinct groups with good separation are evident in PC1.

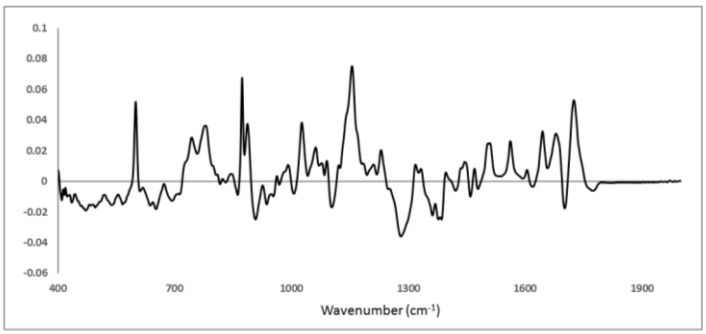

Figure 38. Loadings plot of PCA of spectra of Fraser fir and *Sciadopitys verticillata* resin. Distinct groups with good separation are evident in PC1.

FTIR of Fraser fir. FTIR spectroscopy was used to investigate differences between resins from *S. verticillata* resin because Fraser Fir, a conifer in the family Pinaceae with a range restricted to the higher elevations of western North Carolina, Eastern Tennessee, and southwest Virginia. Fraser fir was not characterized in previous studies (Wolfe *et al*., 2009) (Figure 36).

The first obvious difference in the spectra is the absence of the Baltic shoulder region around 1200 cm^{-1} in Fraser fir. *S. verticillata* resin also has obvious peaks missing from Fraser fir at 1155 and 872cm^{-1}. These peaks are characteristic of the functional group C-O-C and are located at positions consistent with hemicellulose and cellulose. The majority of the peaks found in Fraser fir where also found in *S. verticillata*, with the differences seen being in absorbance intensity levels. Peaks below 800 cm^{-1} were not used in the comparison due to being too saturated with peaks. PCA was used to verify that there was a difference in the resin (Figure 37).

PCA graph showed distinct groupings with good separation with respect to PC1 (Figure 37). 73% of the variability in the resins can be explained by PC1.Loadings plot of PC1 was used to identity five largest peaks located between 700 and 1800 cm^{-1} (Figure 38 and Table 8).

Table 8. Tentatively identified compounds from FF *vs* LN loadings plot. Loadings plot was used to identify pyrolysis products represented by the five largest peaks.

HC vs LN FTIR Loadings Peaks Identified			
Position	**Intensity**	**Functional Group**	**Possible Compound**
872	0.470	C-O-C	Hemicellulose
994	0.309	C=O	Cellulose
1025	0.309	C=O	Cellulose
1155	0.398	C-O-C	Cellulose
1722	0.354	C=O	Ketone, aldehyde

The largest peak in the loadings graph was tentatively identified at 1155 cm^{-1}, an area associated with C-O-C bonding. Strong peaks in this region are characteristic of cellulose. A peak at 872 cm^{-1} was also tentatively identified as representing C-O-C bonds characteristic of hemicellulose.

The three other major peaks at 994, 1025, and 1722 cm^{-1}in the loadings graph was tentatively identified as carboxyl groups (C=O). The 994 and 1025 cm^{-1} peaks are characteristic of cellulose and the 1722 cm^{-1} peak is characteristic of ketones and/or aldehydes.

Differences in the resins were expected, because *S. verticillata* is more closely related to the Cupressaceae resins, and Fraser fir being in the Pinaceae family, should have resin more closely related to other Pinaceae. Interesting is that the major variance between the two resins are associated with common plant sugars.

CHAPTER 4: Summary

Due to the physical characteristics of the resin, it was difficult to use in microbial and chemical studies. DMSO was the only solvent in which the material was completely soluble, but the levels of DMSO required to dissolve the resin were also antimicrobial and cannot be used for reliable antimicrobial tests. Water was determined to be the best liquid for collecting the resin, because the resin precipitated into a pellet that could be autoclaved, lyophilized, and frozen for storage.

GC-MS analysis was used for the detection of potentially antimicrobial volatiles that could be tested against bacteria. Resin contained high concentrations of terpenes, with α-pinene, tricyclene, and β-pinene comprising approximately 95% of the resin's volatiles.

Resin from *Sciadopitys verticillata* is active against several plant pathogenic and food borne bacteria but stimulates population growth of *X. perforans* and pseudomonads. Some strains of *P. fluorescens* can utilize α-pinene as a sole carbon source whereas *Erwinia* is sensitive to the compounds (Scortichini *et al*., 1991). *Bacillus cereus* was not sensitive to levels of α-pinene found in lyophilized resin of *S. verticillata*.

Because pathogens such as *P. syringae* and X. *perforans* are stimulated by this resin, a biopesticide product would be limited to diseases such as fire blight, where pseudomonads are used as biological control agents and the pathogen is sensitive. If pinene is present in the resin at levels predicted by the CGMS analysis, it is likely that other compounds are involved in the activity of the resin. It is possible α-pinene is part of a complex of active components in the resin; however, since levels tested at 1000 times the concentrations shown in GCMS were not as inhibitory as the resin, it is unlikely that α-pinene is the only antimicrobial compound.

FTIR was also used to compare fresh, autoclaved, and lyophilized resins, to compare *S. verticillata* resin to Fraser fir resin, and to determine functional groups in the resin. No differences were detected between fresh, autoclaved, and lyophilized resins other than regions associated with water. There were differences detected between Fraser fir and *S. verticillata* resins, with Fraser fir missing the Baltic shoulder, as have all other tested members of the pine family (Wolfe *et al*., 2009). Other differences detected were that *S. verticillata* has higher content of functional groups characteristic of cellulose, hemicellulose, ketones, and aldehydes. Functional groups detected were consistent with previous reports of *S. verticillata* resin as being more similar to Cupressaceous resins than to Pineaecous resins (Tappert *et al*., 2011).

NMR was used to detect and tentatively identify the major classes of resin components. Resin contained aldehydes, aromatics, olefins, alkoxy groups, ethers, alkyls, and carbonyls.

Pyrolysis GCMS was used to detect and tentatively identify the major pyrolysis degradation products of the resin and to compare resins collected from six source trees. Eight pyrolysis products comprised at least 1% of the total peak area and combined represented approximately 38% of the total peak area. These eight pyrolysis degradation products can be grouped into six steroid-like and two communal-like groups, with the most abundant degradation product being the steroid 3-ethyl-3-hydroxy-(5à)-Androstan-17-one (13%).

Comparison of resin from six different source trees indicated that four of the resins were remarkably similar. Differences between the remaining resins were possibly a result of the environment in which the tree was growing, particularly the level of sun. Differences detected were functional groups normally associated with sugars and carbon dioxide, and thus might have been associated with photosynthetic activity. Two trees were genetically identical. Differences

detected in these resins were relatively low in abundance (1% or less) lower molecular weight volatile degradation products that, with the exception of α-pinene, were none of the major antimicrobial pyrolysis degradation products detected earlier.

This is believed to be the most comprehensive research of the biological activity and chemical characterization of *S. verticillata* to date. Further research into the resin will need to be conducted to determine exactly which combinations of resin components are antimicrobial and probiotic. Other species of bacteria need to be tested for effect of resin on population growth. Research into possible antifungal and pesticide activities need to be conducted to fully determine the resin's potential. The resin is such a complex mixture of compounds that further investigations using more advanced chemical analytical techniques will have to be conducted to fully characterize the resin's chemistry and potential future uses. Of course, the problem with the availability and expense of this species to researchers and industry may also need to be addressed if the resin is determined to be unique in bioactivity or a source of valuable chemicals for industry and/or medicine.

BIBLIOGRAPHY

1) Khalil, A.; Dababneh, B. F.; Al-Gabbiesh, A. H. Antimicrobial activity against pathogenic microorganisms by extracts from herbal Jordanian plants. *J. Food Agric. Env*. 2009, *7*, 103-106.
2) Silva, N. C.; Fernandes, J. A. Biological properties of medicinal plants: a review of their antimicrobial activity. *J. Venom Anim. Toxins*. 2010, *16*, 402-413.
3) García-Lomillo, J.; González-SanJosé, M. L.; Pino-García, D. A.; Rivero-Pérez, M. D.; Muñiz-Rodríguez, P. Antioxidant and antimicrobial properties of wine byproducts and their potential uses in the food industry. *J. Agric. Food Chem.* 2014, *62*, 12595-12602.
4) Devcich, D. A.; Pedersen, I. K.; Petrie, K. J. You eat what you are: modern health worries and the acceptance of natural and synthetic additives in functional foods. *Appetite* 2007, *48*, 333-337.
5) Stockwell, V. O.; Duffy, B. Use of antibiotics in plant agriculture. *Sci. Technol. Rev.* 2012, *31*, 199-210.
6) Cowan, M. M. Plant products as antimicrobial agents. *Clin. Microbiol. Rev.* 1999, *12*, 564-582.
7) Tiwari, B. K.; Valdramidis, V. P.; O'Donnell, C. P.; Muthukumarappan, K.; Bourke, P.; Cullen, P. J. Application of natural antimicrobials for food preservation. *J. Agric. Food Chem.* 2009, *57*, 5987-6000.
8) Shults, E. E.; Mironov, M. E.; Kharitonov, Y. V. Furanoditerpenoids of the labdane series: occurrence in plants, total synthesis, several transformations, and biological activity. *Chem. Of Natural Prod.* 2014, *50*, 2-21.
9) Widsten, P.; Cruz, C. D.; Fletcher, G. C.; Pajak, M. A.; McGhie, T. K. Tannins and extracts of fruit byproducts: antibacterial activity against foodborne bacteria and antioxidant capacity. *J. Agric. Food Chem.* 2014, *62*, 11146-11156.
10) Cantrell, C. L.; Dayan, F. E.; Duke, S. O. Natural products as sources for new pesticides. *J. Nat. Prod.* 2012, *75*, 1231-1242.
11) Wolfe, A. P.; Tappert, R.; Muehlenbachs, K.; Boudreau, M.; McKellar, R. C.; Basinger, J. F. A new proposal concerning the botanical origin of Baltic amber. *Proceedings of the Royal Society B: Biological Sciences.*2009, *276*, 3403-3412.
12) Langenheim, J. H. Resin producing plants. *Plant Resins,* edition 1; Timber Press Inc.: Portland, OR. 2003, 51-98.
13) Tappert, R.; Wolfe, A. P.; McKellar, R. C.; Tappert, M. C.; Muehlenbachs, K. Characterizing modern and fossil gymnosperm exudates using micro-Fourier infrared spectroscopy. *Int. J. Plant Sci*. 2011, *172*, 120-138.
14) Croteau, R.; Kutchan, T. M.; Lewis, N. G. Natural products. *Biochem. Mol. Bio. Plants* 2000, *11*, 1250-1318. Missing volume
15) McGarvey, D. J.; Croteau, R. Terpenoid metabolism. *Plant Cell* 1995, *7*, 1015-1026.
16) Trapp, S.; Croteau, R. Defense resin biosynthesisin conifers, *Annu. Rev. Plant Physiol. Plant Mol*, Biol. 2001, *52*, 689-724.
17) Sadowski, E. M.; Schmidt, A. R.; Kunzman, L.; Grohn, C.; Seyfullah, L. J. *Sciadopitys* cladodes from Eocene Baltic amber. *Bot. J. Linn. Soc*. 2013, *180*, 258-268.
18) Eckenwalder, J. E. *Conifers of the world. The complete reference*. Timber Press. Portland, OR, 2009, 580-583.

19) Florin, R. Untersuchungenzurstammesgeschichte der Coniferales und Cordaitalesmorphologie und epidermisstruktur der assimilationsorganebei den rezentenkoniferen. *KungligaSvenskaVetenskapsakademiensHandlingar*. 1931, *10*, 1-588.
20) Farjon, A. A monograph of Cupressaceae and *Sciadopitys*. *Kew Royal Botanic Gardens*. 2005, 1-12.
21) Dörken, V. M.; Stützel, T. Morphology and anatomy of anomalous cladodes in *Sciadopitys verticillata*Siebold&Zucc. (Sciadopityaceae). *Trees.* 2011, *25*: 199-213.
22) Li, J.; Gao, L.; Chen, S.; Tao, K.; Su, Y.; Wang, T. Evolution of short inverted repeat in cupressophytes, transfer of accD to nucleus in Sciadopitys verticillata and phylogenetic position of Sciadopityaceae. *Sci. Reports*. 2016, *6*, 1-12.
23) Yang, Z. Y.; Ran, J. H.; Wang, X. Q. Three genome-based phylogeny of Cupressaceae s.l.: further evidence for the evolution of gymnosperms and Southern Hemisphere biogeography. *Mol. Phylogenet. Evol.* 2012, *64*, 452-470.
24) Crisp, M. D.; Cook, L. G. Cenozoic extinctions account for the low diversity of extant gymnosperms compared with angiosperms. *New Phytol*. 2011, *192*, 997–1009.
25) Chapuisat, M.; Oppliger, A.; Magliano, P.; Christie, P. Wood ants use resin to protect themselves against pathogens. *Proc. R. Soc. B.* 2007, *274*, 2013-2017.
26) Nosova, N.; Kiritchkova , A. Mesozoic conifer genus SciadopityoidesSveshnikova (Miroviaceae). *Rev. Palaeobot. Palynology*, 2015, *221*, 1-21.
27) Choudhary, A.; Rao, P. T.; Sharma, S. Removal of fluoride from drinking water by quarternaryaminated resins from saw-dust. *Eur. Chem. Bulletin,* 2014, *3,* 242-246.
28) Yates, D. I.; Earp, B. L.; Walker, E. S.; Levy, F. Propagation of Sciadopitys verticillata (Thunb.) Sieb. &Zucc. by stem cuttings and properties of its latex-like sap. *Hortscience* 2006, *41,* 1662-1666.
29) Phillips, O. Ficusinsipida (Moraceae) ethanobotany of an Amazonian antihelmintic, *Econ. Bot*., 1990, *44*, 534-536.
30) Mills, J. S.; White, R.; Gough, L. The chemical composition of Baltic amber. *Chem. Geo*. 1984, *47*, 15-39.
31) Rabi, I. I.; Zacharias, J. R.; Millman, S.; Kusch, P. A new method of measuring nuclear magnetic moment. *Phys. Rev*. 1938, *53*, 318-327.
32) Lopes, T. I. B.; Ribeiro, M.; Ming, C. C.; Grimaldi, R.; Gonçalves, L .A. G.; Marsaioli, A. J. Comparison of the regiospecific distribution from triacylglycerols after chemical and enzymatic interesterification of high oleic sunflower oil and fully hydrogenated high oleic sunflower oil blend by carbon-13 nuclear magnetic resonance. *Food Chem*. 2016, *212*, 642-647.
33) Martin-Pastor, M.; Guitian, E.; Riguera, R. Joint NMR and solid-phase microextraction−gas chromatography chemometric approach for very complex mixtures: grape and zone identification in wines. *Anal. Chem*. 2016, *88*, 6239-6246.
34) Andrikopoulos, N. K. Chromatographic and spectroscopic methods in the analysis of triacylglycerol species and regiospecific isomers of oils and fats. *Crit. Rev. Food Sci. and Nutr*. 2002, *42*, 473-505.
35) Megeressa, M.; Bisrat, D.; Mazumder, A.; Asres, K. Structural elucidation of some antimicrobial constituents from the leaf of *Aloe trigonantha*. BMC *comp. Alt. Med.* 2015, *15*, 270-275.

36) Dghim, F.; Bouazizb, M.; Mezghanic, I.; Boukhrisc, M.; Nefatti, M. Laticifers identification and natural rubber characterization from the latex of *Periplocaangustifolia* (Apocynaceae). *Flora* 2015, *217*, 90-98.
37) Agrawal, A. A. Konno, K. Latex: A model for understanding mechanisms, ecology, and evolution of plant defense against herbivory, *Annu. Rev Ecol. Syst.* 2009, *40*, 311-331.
38) Liggieri, C.; Arribere, M. C.; Trejo, S. A.; Canals, F.; Aviles, F. X.; Priolo, N. S. Purification and biochemical characterization of *Asclepiascurassaviza* L. *Protein J*. 2004, *23*, 403-411.
39) Kawase, D.; Tsumura, Y.; Tomaru, N.; Seo, A.; Yumoto, T. Genetic structure of an endemic conifer, *Sciadopitys verticillata* (Sciadopityaceae), by using microsatellite markers. *J. Heredity* 2010, *101*, 292-297.
40) Dee, M. M.; Quigley, N. B.; Ownley, B. H. Micro-dilution plating technique for assessing population counts of microorganisms. *Phytopathology* 1995, *85*, 1204-1206.
41) Hoerr, V.; Duggan, G. E.; Zbytnuik, L.; Poon, K. K.; Grobe, C.; Neugebauer, U.; Methling, K.; Loffler, B.; Vogel, H. J. Characterization and prediction of the mechanism of action of antibiotics through NMR metabolomics. *BMC Microbiology* 2016, *16*, 1-14.
42) Dhar, P.; Chan, P. Y.; Cohen, D. T.; Khawam, F.; Gibbons, S.; Snyder-Leiby, T.; Dickstein, E.; Rai, P. K.; Watal, G. Synthesis, antimicrobial evaluation, and structure activity relationship of α-pinene derivatives. *J. Agric. Food Chem*. 2014, *62*, 3548-3552.
43) Maškovic, P.; Radojkovic, M.; Ristic, M.; Slavica, S. Studies on the antimicrobial and antioxidant activity and chemical composition of the essential oils of *Kitaibeliavitifolia*. *Nat. Prod. Comm.* 2013, *8*, 667-670.
44) Bozin, B.; Mimica-Dukic, N.; Samojlik, I.; Jovin, E. J. Antimicrobial and antioxidant properties of rosemary and sage (*Rosmarinus officinalis* L. and *Salvia officinalis* L., Lamiaceae) essential oils. *J. Agric. Food Chem*. 2007, *55*, 7879-7885.
45) Iscan, G.; Kirimer, N.; Kurkcuoglu, M.; Baser, K. H. C.; Demirci, F. Antimicrobial screening of *Menthapiperita* essential oils. *J. Agric. Food Chem*. 2002, *50*, 3943-3946.
46) Dadalioglu, I.; Evrendilek, G. A. Chemical compositions and antibacterial effects of essential oils of Turkish oregano (*Origanumminutiflorum*), bay laurel (*Laurusnobilis*), Spanish lavender (*Lavandulastoechas* L.), and fennel (*Foeniculum vulgare*) on common foodborne pathogens. *J. Agric. Food Chem*. 2004, *52*, 8255-8260.
47) Lis-Balcnina, M.; Ochockab, R. J.; Deansc, S. G.; Asztemborskad, M.; Differences in bioactivity between the enantiomers of α-pinene. *J. Essent. Oil Res*. 1999, *11*, 393-397.
48) Nikolić, B.; Tesević, V.; Ethordević, I.; Marin, P. D.; Bojović, S. Essential oil variability in natural populations of *Piceaomorika*, a rare European conifer. *Chem. Biodivers*. 2009, *2*, 193-203.
49) Rajaian, H; Nazer, A. H. K. *In vitro* antimicrobial effects of tricyclines A, B and C against various microorganisms isolated from animals. *J. Appl. Anim. Res.*1999, *15*, 117-120.
50) Geron, C., Rasmussenb, R.; Arntsc, R. R.; Guentherd, A. A review and synthesis of monoterpene speciation from forests in the United States. *Atmos. Environ*. 2000, *34*, 1761-81.

51) Mahajan, P.; Batish, D. R.; Singh, H. P.; Kohli, R. K. *β*-Pinene partially ameliorates Cr(VI)-inhibited growth and biochemical changes in emerging seedlings. *Plant Growth Regul.* 2016, *79*, 243-249.
52) Singsaas, E. L. Terpenes and the thermotolerence of photosynthesis. Forum commentary. *New Phytol.* 2000, *146*, 1-4.
53) Loreto, F.; Mannozzi, M.; Nascetti, M. C.; Ferranti, F.; Pasqualini, S. Ozone quenching properties of isoprene and its antioxidant role in plants. *Plant Physiol*. 2001, *126*, 993-1000.
54) Barrére, G. C.; Barber, C. E.; Daniels, M. J. *Int. J. Biol. Macromol.* 1986, *8*, 372-374.
55) Haas, D.; Keel, C. Regulation of antibiotic production in root-colonizing *Pseudomonas* spp. and relevance for biological control of plant disease. *Annu. Rev. Phytopathol*. 2003, *41*, 117-153.
56) Cheng, Z. W.; Chen, J. M.; Yu, J. M.; Li, S. S. Structural characterization and property analysis of surface-active substance accumulated during biodegradation of hydrophobic α-pinene by *Pseudomonas fluorescens*. Water Air Soil Pollut. 2013, 224, 1457-1461.
57) Wageningen, Y. S.; Van der Wolf, International biointeractions and plant health. *J. Plant res.* 2004, *12*, 68-72.
58) Schoeni, J. L.; Wong, A. C. L. *Bacillus cereus* food poisoning and its toxins. *J. Food Protec*. 2005, *68*, 636-648.
59) Meccia, J.; Rojas, L. B.; Velasco, J.; Díaz, T.; Usubillaga, A.; Arzola, J. C.; Ramos, S. Chemical composition and antibacterial activity of the essential oil of *Cordia verbenaceae* from the Venezuelan Andes. *Nat. Prod. Com.* 2009, *8*, 1119-1122.
60) Hsueh, P. R.; Teng, L. J.; Yang, P. C.; Pan, H. L.; Ho, S. W.; Luh, K. T. Nosocomial pseudoepidemic caused by *Bacillus cereus* traced to contaminated ethyl alcohol from a liquor factory. *J. Clinic. Microbiol*. 1999, *37*, 2280-2284.
61) Lang, J.; Vigouroux, A.; Planamente, S.; Sahili, E. A.; Blin, P.; Aumont-Nicaise, M.; Dessaux, Y.; More, S.; Faure, D. *Agrobacterium* uses a unique ligand-binding mode for trapping opines and acquiring a competitive advantage in the niche construction on plant host. *PLOS Biol.* 2014, *79*, 109-112.
62) Scortichini, M.; Rossi, M. P. Preliminary in vitro evaluation of the antimicrobial activity of terpenes and terpenoids towards Erwinia amylovora (Burrill). *J. Bacterol.* 1991, *71*, 108-112.
63) Savithiry, N.; Gage, D.; Fu, W.; Orielet, P. Degradation of pinene by Bacillus pallidus BR425. *Biodegradation.* 1998, *9*, 337-341.
64) Adams, A. S.; Boone, C. K.; Bohlmann, J.; Raffa, K. F. Responses of bark beetle-associated bacteria to host monoterpenes and their relationship to insect life histories. *J. Chem. Ecol.* 2011, *37*, 808-817.
65) McNaught A. D. Compendium of Chemical Terminology. *Blackwell Scientific Publications*, Oxford Press. 1997, 4-9.
66) Kohlpaintner, C.; Schulte, M.; Falbe, J.; Lappe, P.; Weber, J. *Aldehydes, Aliphatic. Ullmann's Encyclopedia of Industrial Chemistry*. 2008, 68-142.
67) Larson, J. C. Polycyclic aromatic hydrocarbons – Occurrence in foods, dietary exposure and health effects. *Eu. Com. Sci. Com. on Food*. 2002, *9*, 23-25.

68) Larsson, B. K.; Sahlberg, G. P.; Eriksson, A. T.; Busk, L. A. Polycyclic aromatic hydrocarbons in grilled food. *J. Agric. Food Chem*. 1983, *31*, 867-873.
69) Augustin, J. M.; Kuzina, V.; Andersen, S. B.; Bak, S. Molecular activities, biosynthesis and evolution of triterpenoid saponins. *Phytochemistry*, 2011, *72*, 435–57.
70) Thimmappa, R.; Geisler, K.; Louveau, T.; O'Maille, P.; Osbourn, A. Triterpene biosynthesis in plants. *Annu. Rev. Plant Biol*. 2014, *65*, 225-57.
71) Wade**,** L. G. *Organic Chemistry* (6th ed.), Pearson Prentice Hall. 2006, 279.
72) Rodriguez-Corres, K. C.; Lima, J. C.; Fett-Netto, A. G. Pine oleoresin: tapping green chemicals, biofuels, food production, and carbon sequestration from multipurpose trees. *Food Energy Sec*. 2012, *1*, 81-93.
73) Mallavadhani, U. V.; Sahoo, L.; Kumar, K. P.; Murty, U. S. Synthesis and antimicrobial screening of some novel chalcones and flavanones substituted with higher alkyl chains. *Med. Chem. Res*. 2013, *4*, 61-68.
74) Xu, F.; Jianming, Y.; Tesso, T.; Dowell, F.; Wang, D. Qualitative and quantitative analysis of lignocellulosic biomass using infrared techniques: a mini-review. *J. Appl. Energy* 2013, 104, 801-809.
75) Poulin, J.; Helwig, K. Inside amber: the structural role of succinic acid in class 1a and class 1d resinite. *Anal. Chem*. 2012, *86*, 7428-7435.
76) Hasegawa, O. F.; Hayasaki, Y. M.; Noda, K. Clinical and bacteriological studies of new antimicrobial agents. *J. Obst. Gyn*. 1986, *6*, 36-39.
77) Jegajeevanram, P.; Alhaji, N. M. I.; Velavan, S. Identification of insecticidal components of mango ginger rhizome and *Tageteserecta* flower extracts by GC-MS analysis. *Chem. Pharm. Anal*. 2014, *1*, 203-207**.**
78) Takemura, M.; Endo, S.; Matsunaga, T.; Soda, M.; Zhao, H. T.; El-Kabbani, O.; Tajima, K.; Iinuma, M.; Hara, A. Selective inhibition of the tumor marker aldo-keto reductase family member 1B10 by oleanolic acid. *J. Nat. Prod.* 2011, *74*, 1201-1206.
79) Al-Masoudi, N. A.; Kadhim, R. A.; Abdul-Rida, N. A. New biaryl-chalcone derivatives of pregnenolone via Suzuki-Miyaura cross-coupling reaction. Synthesis, CYP17 hydroxylase inhibition activity, QSAR, and molecular docking study. *Steroids* 2015, *101*, 43-50.
80) Ndukwe, I. G.; Amupitan, J. O.; Zhao, Y. Isolation and characterization of 3, 5, 6-trihydroxy-7-octyl-5, 6-dihydro-1-naphthalene carboxylic acid from the stem methanolic extract of *Vitellaria paradox*. *J. Med. Plant Res*. 2007, *3*, 60-62.

87) Sudha, T. J.; Chidambarrampillai, S.; Mohan, V. R. GC-MS Analysis of bioactive components of aerial parts of *Kirganeliareticulata* (Eupohrbiaceae). *Curr. Chem. Pharm. Sc*. *3*, 2013, 113-122.
88) Roy, A.; Saraf. S. Limonoids: overview of significant bioactive triterpenes distributed in plants kingdom. *Biol. Pharm. Bull*. 2006 *29*, 191-201.
89) Jacob, R.; Hasegawa, S.; Manners, G. The Potential of citrus limonoids as anticancer agents. *Perish. Hand. Quart*. 2000, *102*, 6-8.
90) Auldridge, M. E.; McCarty, D. R.; Klee, H. J. Plant carotenoid cleavage oxygenases and their apocarotenoid products. *Cur. Op. Plant Biol.* 2006, *9*, 315-321.

91) Panzella, L.; Manini, P.; Napolitano, A.; d'Ischia, M. Free radical oxidation of E-retinoic acid by the Fenton reagent: competing epoxidation and oxidative breakdown pathways and novel products of 5,6-epoxyretinoic acid transformation, *Chem. Res. Toxicol.* 2004, *17*, 1716-1724.
92) Campbell, M. L. Cyclohexane in *Ullmann's Encyclopedia of Industrial Chemistry,* John Wiley and Sons, Ltd. 2000, 244-265.
93) Borg-Karlson, A. K.; Norin, T.; Talvitie, A. Configurations and conformations of torreyol δ-cadinol, α-cadinol, T-murolol and T-cadinol. *Tetrahedron.* 1831, *37(2)*, 425–430.
94) Kütt, A.; Movchun, V.; Rodima, T.; Dansauer, T.; Rusanov, E. B.; Leito, I.; Kaljurand, I.; Koppel, J.; Pihl, V.; Koppel, I.; Ovsjannikov, G.; Toom, L.; Mishima, M.; Medebielle, M.; Lork, E.; Röschenthaler, G.; Koppel, I. A.; Kolomeitsev, A. A. Pentakis (trifluoromethyl) phenyl, a sterically crowded and electron-withdrawing group: synthesis and acidity of pentakis (trifluoromethyl) benzene, -toluene, -phenol, and -aniline". *J. of Org. Chem*. 2008. *73*, 2607-20.
95) Hanscha, C.; McKarns, S. C.; Smith, C. J; Doolittle, D. J. Comparative QSAR evidence for a free-radical mechanism of phenol-induced toxicity. *Chemico-Biol. Inter*. 2000, *127*, 61-72.
96) Scortichini, M.; Rossi, M. P. Preliminary *in vitro* evaluation of the antimicrobial activity of terpenes and terpenoids towards *Erwinia amylovora* (Burrill). *J. Appl. Bac*. 1991, *71*, 109-112.

APPENDICES

APPENDIX 1

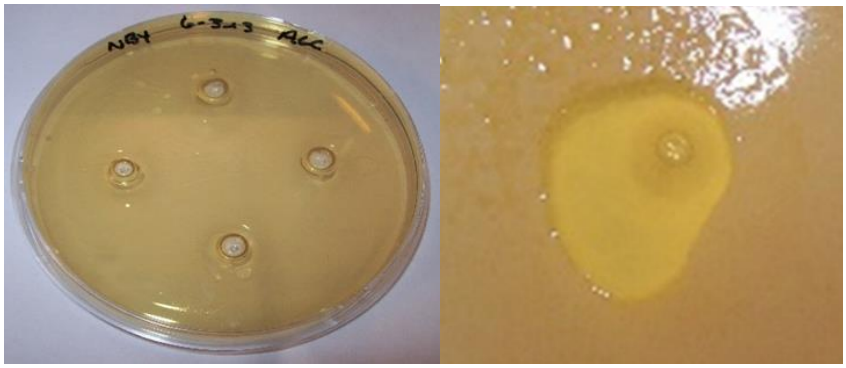

Figure A.1. The overlay method.

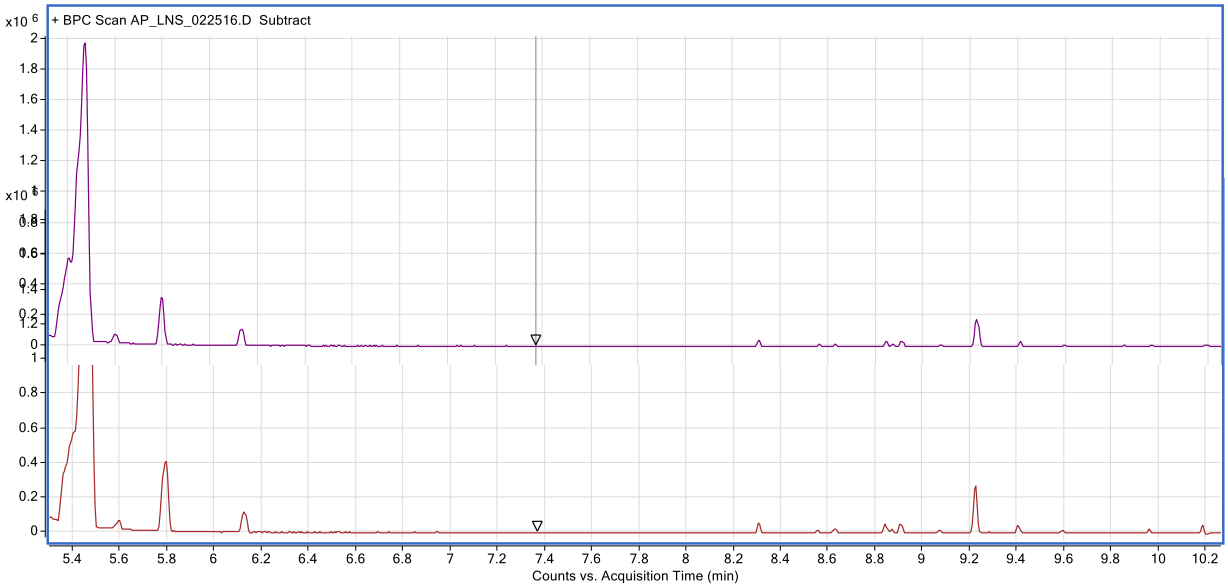

Figure A.2. GCMS spectra of resin. Volatiles of summer- winter-collected resin of *S. verticillata* resin with solvent peaks excluded.

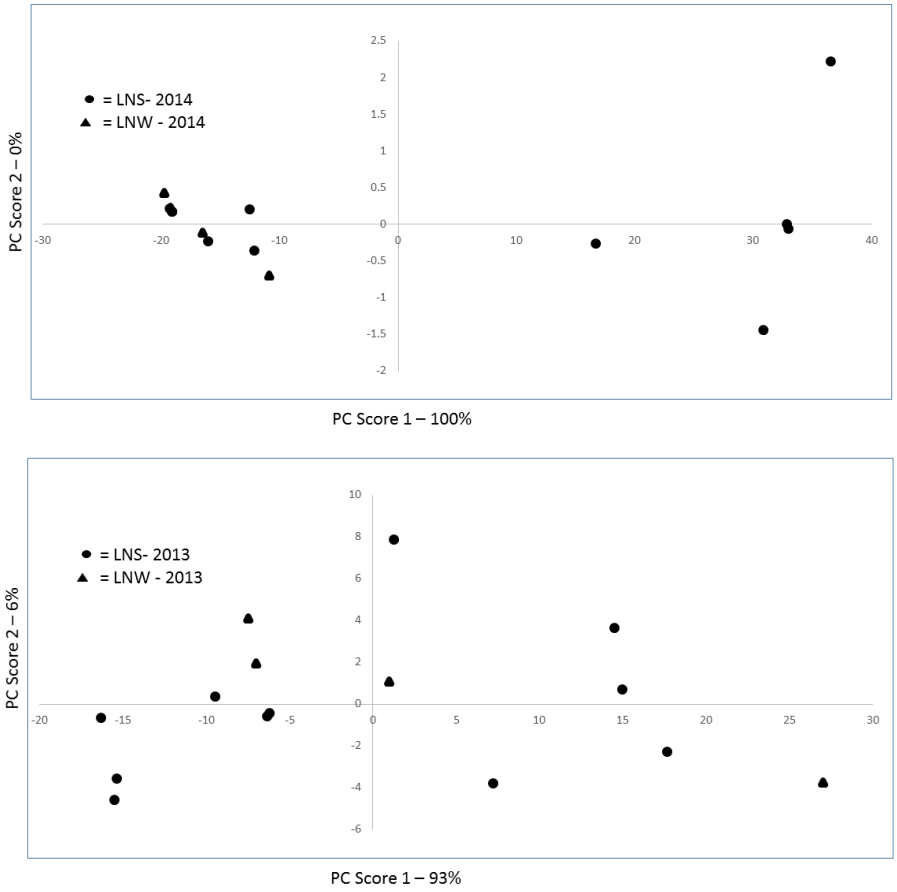

Figure A.3. PCA score plots of composition of resins collected in Summer (June/July) and Winter (February/March) 2013 and 2014. The lack of grouping by collection period suggests that no compositional differences were detected in different seasons.

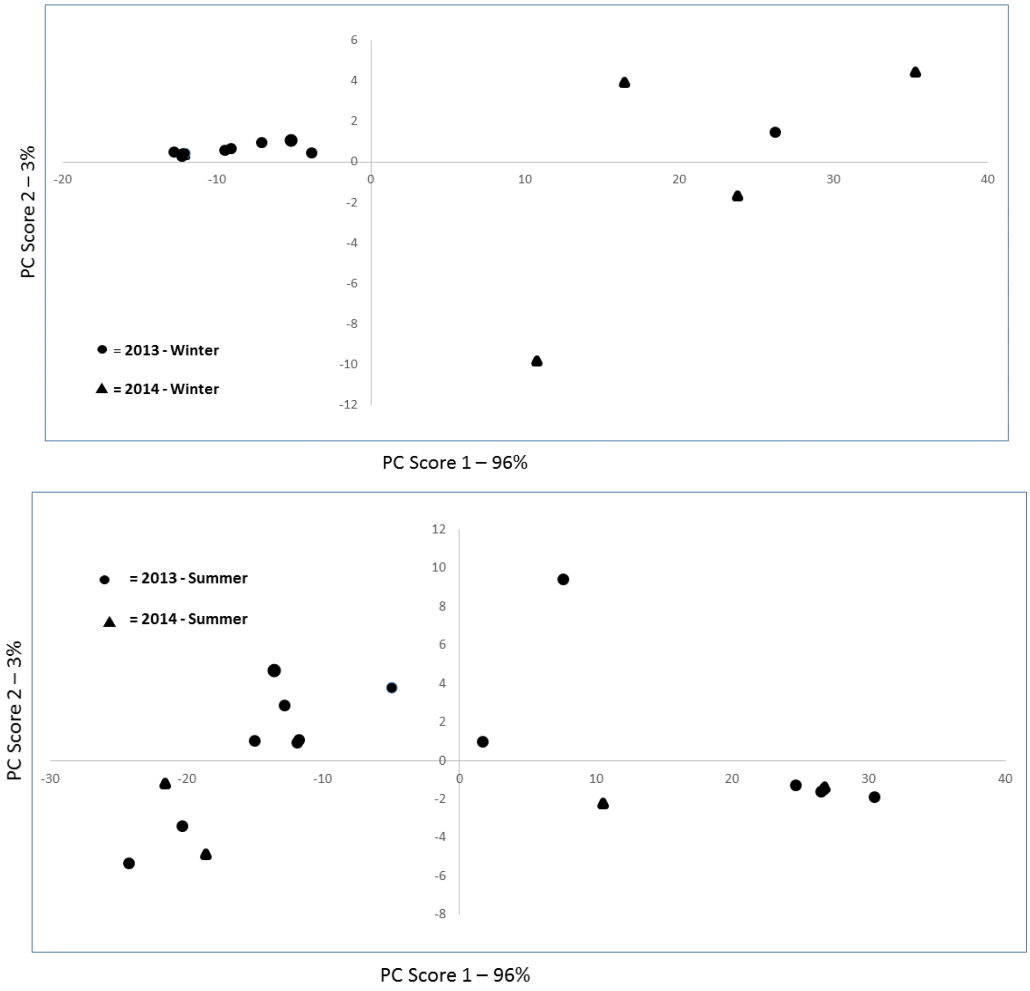

Figure A.4. PCA score plots of composition of resins collected in 2013 and 2014 in the Summer (June/July) and Winter (February/March) 2013. The lack of grouping by year suggests that no compositional differences were detected in different years.

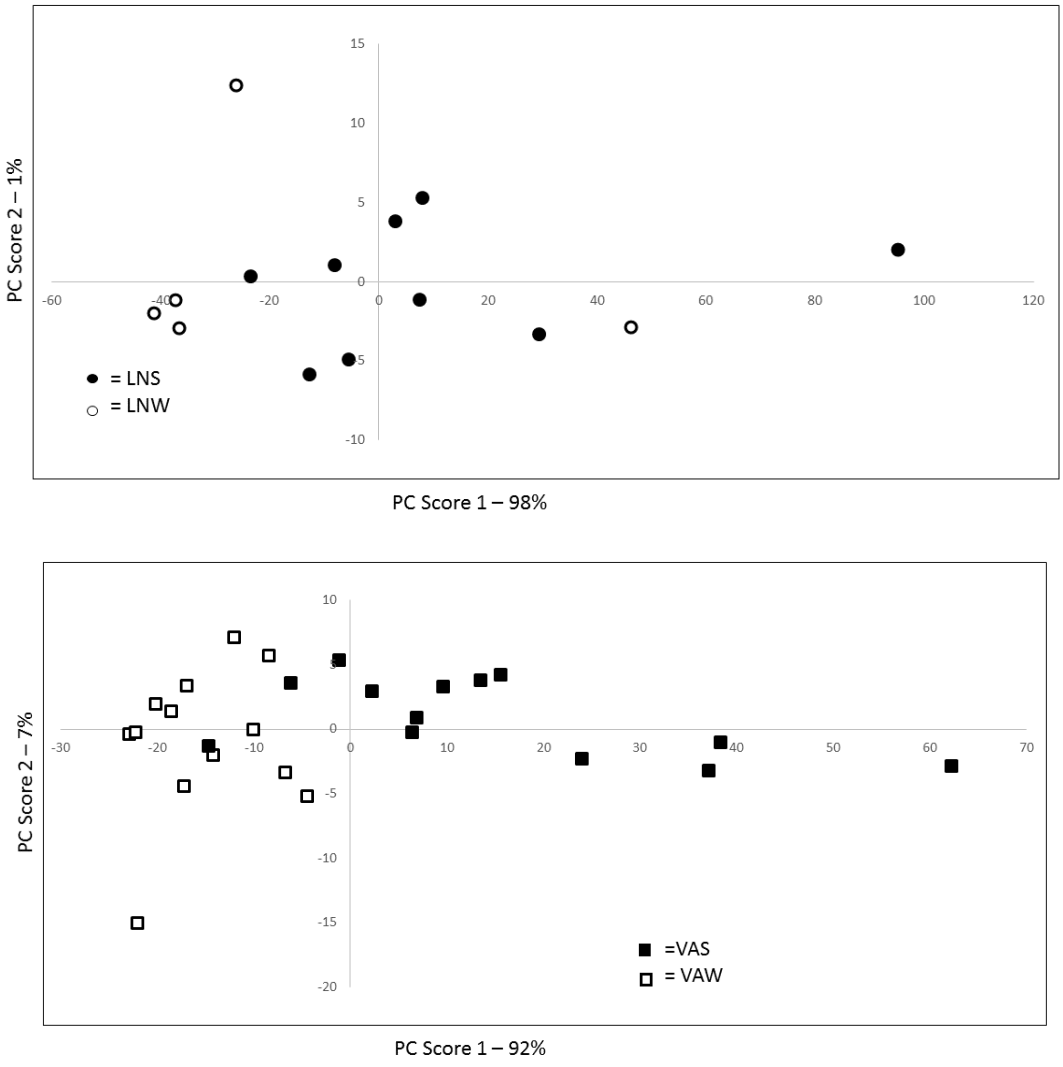

Figure A.5. Effect of season on resin chemistry at two locations (LN and VA). FTIR spectra were analyzed by Principal Component Analysis. The lack of grouping by collection period suggests that no compositional differences were detected at each site in the two seasons.

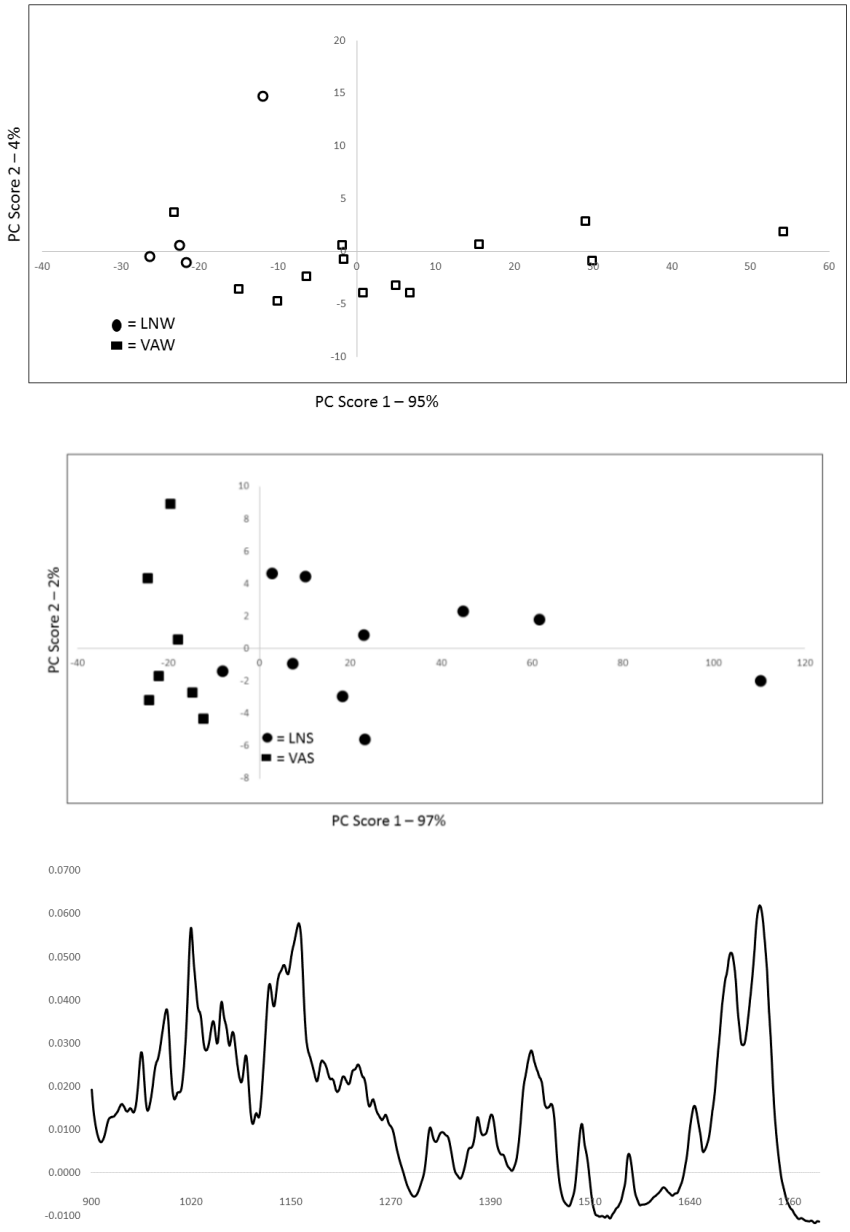

Figure A.6. Effect of location on resin chemistry in two seasons (Winter and Summer). FTIR spectra were analyzed by Principal Component Analysis. The lack of grouping in the PCA scores plot by collection period suggests that no compositional differences were detected between the locations in winter. Scatter plot formed distinct sample groupings, indicating that samples collected in summer at LN are different than those at VA, and that 97% of the variance can be explained by principle component 1. Loadings plot of the first principle component (See Figure 24) from FTIR spectra of *Sciadopitys verticillata* resin. Loadings was used to identify functional groups responsible for variance between the lyophilized and nonlyophilized samples.

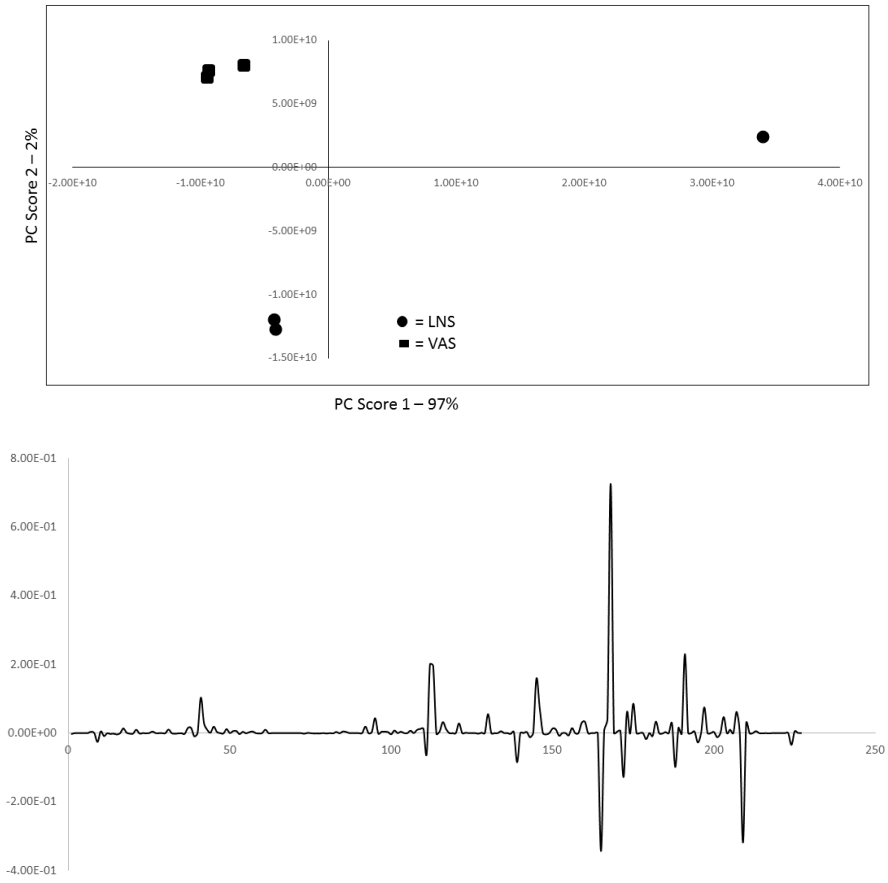

Figure A.7. Effect of location on resin chemistry in Summer 2014. Pyrolysis GCMS data were analyzed by Principal Component Analysis. Since scatter plots formed distinct sample groupings, samples collected in summer at LN are different than those at VA, and that 97% of the variance can be explained by principle component 1. Loadings plot of the first and second principle component were used to identify pyrolysis productsresponsible for variance between the lyophilized and nonlyophilized samples.

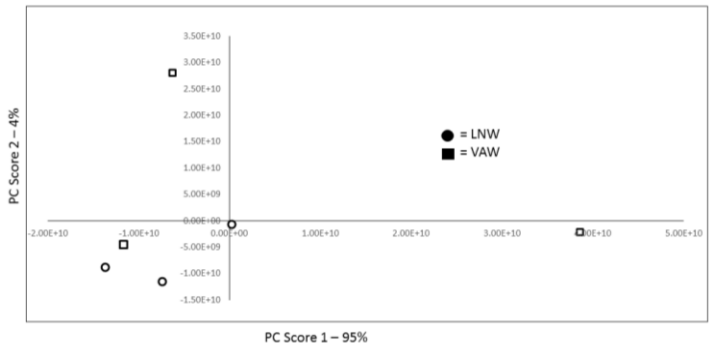

Figure A.8. Effect of location on resin chemistry in Winter 2014. Pyrolysis GCMS data were analyzed by Principal Component Analysis. Since scatter plots did not form distinct sample groupings, samples are considered not different.

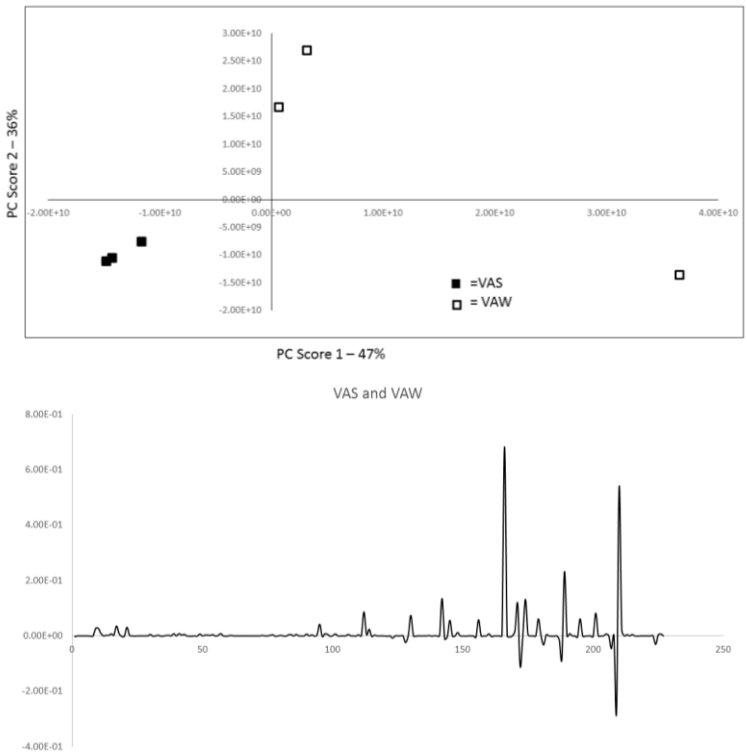

Figure A.9. Effect of season on resin chemistry in VA samples (2014). Pyrolysis GCMS data were analyzed by Principal Component Analysis. Since scatter plots formed distinct sample groupings, samples collected in are different than winter, and that 47% of the variance can be explained by Principle Component 1. Loadings plot of the first principle component was used to identify pyrolysis products responsible for variance between the lyophilized and nonlyophilized samples.

Table A.1. Environmental conditions for Johnson City, TN during the periods of resin collection.

	Winter (February/March)		Summer (June/July)	
Parameter	**2013**	**2014**	**2013**	**2014**
Day Length (h)	11.4	11.4	14.4	14.6
Temperature (F	40.0	42.0	74	74
Rainfall (in)	3.24	2.76	6.18	5.98
	Winter (February/March)		**Summer (June/July)**	
Parameter	**2013**	**2014**	**2013**	**2014**
Day Length (h)	11.4	11.4	14.4	14.6
Temperature (C)	4.4	5.5	23.3	23.3
Rainfall (cm)	8.23	7.02	15.7	15.2

Table A.2. Compounds Identified in Resin. Resin compounds identified using the MassHunter software to search the NIST02 library of mass spectra and listed by percent of total peak areas (Largest to smallest). Not Present (NP) indicates that the compound was not identified in the resin sample.

Chemical Name	Retention Time	Summer		Winter	
		Score	% Peak Area	Score	% Peak Area
1R-α-Pinene	5.474	92.73	**73.552**	92.35	**82.003**
Tricyclene	5.399	88.18	**16.977**	**NP**	**0.000**
β-Pinene	5.794	81.17	**5.613**	83.4	**7.656**
β-cubebene	9.222	92.4	**2.540**	77.36	**3.635**
D-limonene	6.132	87.84	**1.634**	88.21	**1.784**
Camphene	5.600	81.46	**0.816**	80.25	**0.789**
Contaminant (Silica gel)	10.189		**0.796**		**0.900**
3 7 α-terpinyl propionate	8.306	78.23	**0.432**	80.23	**0.579**
β-cubebene	8.907	82.07	**0.388**	84.98	**0.541**
β-cubebene	8.844	84.68	**0.384**	86.65	**0.586**
1-Naphthalenol	9.405	76.91	**0.316**	78.49	**0.472**
γ-Cadinene	8.627	84.76	**0.171**	88.42	**0.267**
Caryophyllene	8.867	87.05	**0.113**	88.26	**0.195**
Copaene	8.558	81.98	**0.110**	79.42	**0.159**
β-Ionone	9.954	71.69	**0.104**	74.25	**0.181**
NO Name	9.073	70.43	**0.045**	**NP**	**0.000**
7 a-terpinyl propionate	9.588	62.92	**0.041**	69.18	**0.124**
Tetracyclo[5.3.1.1(2,6).0(4,9)]	9.845	60.52	**0.033**	**NP**	**0.000**
-Cadinene	9.067	NP	**0.000**	93.00	**0.128**

Table A.3. *Xanthomonas perforans* SAS output. Statistical results (SAS) comparing growth of *Xanthomonas perforans* treated with varying amounts of resin from different seasons.

	Xanthomonas perforans			
Resin	**Summer**		**Winter**	
0-25	0.0025	Sig Diff	0.0037	Sig Diff
0-50	0.0195	Sig Diff	0.0209	Sig Diff
0-100	0.0047	Sig Diff	0.0590	Sig Diff
25-50	0.9034	No Diff	0.9494	No Diff
25-100	0.8023	No Diff	0.7954	No Diff
50-100	0.9994	No Diff	0.9815	No Diff

Table A.4. *Xanthomonas perforans* SAS least square means.

X. perf.		**Summer Fresh**				**Winter Fresh**		
Resin Amount	**LSM**		**% Compared to Control**	**% Effect**	**LSM**		**% Compared to Control**	**% Effect**
0	9.333	b	1.00	0.00	131.198	b	1.00	0.00
25	25.833	a	2.77	-1.77	179.802	a	1.37	-0.37
50	22.500	a	2.41	-1.41	172.179	a	1.31	-0.31
100	22.000	a	2.36	-1.36	166.821	a	1.27	-0.27

Table A.5. *Pseudomonas florescens* SAS output. Statistical results (SAS) comparing growth of *Pseudomonas florescens* treated with varying amounts of winter collected resin.

	Pseudomonas fluorescens					
Resin	**Summer Fresh**	**Summer Fresh**	**Winter Fresh**	**Winter Fresh**	**Summer Stored**	**Summer Stored**
0-25	0.9219	No Diff	<.0001	Sig Diff	<.0001	Sig Diff
0-50	<.0001	Sig Diff	<.0001	Sig Diff	<.0001	Sig Diff
0-100	<.0001	Sig Diff	<.0001	Sig Diff	<.0001	Sig Diff
25-50	<.0001	Sig Diff	<.0001	Sig Diff	<.0001	Sig Diff
25-100	<.0001	Sig Diff	<.0001	Sig Diff	<.0001	Sig Diff
50-100	<.0001	Sig Diff	<.0001	Sig Diff	<.0001	Sig Diff

Table A.6. *Pseudomonas florescens* least square means.

P. fluor.	**Summer Fresh**				**Winter Fresh**				**Summer Stored**			
Resin Amount	**LSM**		**% Compared to Control**	**% Effect**	**LSM**		**% Compared to Control**	**% Effect**	**LSM**		**% Compared to Control**	**% Effect**
0	10.625	c	1.00	0.00	47.8148	d	1.00	0.00	83.7531	d	1.00	0.00
25	14.375	c	1.35	-0.35	115.204	c	2.41	-1.41	144.315	c	1.72	-0.72
50	80.125	b	7.54	-6.54	204.167	b	4.27	-3.27	256.235	b	3.06	-2.06
100	201.667	a	18.98	-17.98	282.815	a	5.91	-4.91	326.765	a	3.90	-2.90

Table A.7. Statistical results (SAS) comparing growth of *Pseudomonas syringae* treated with varying amounts of resin from different seasons.

Pseudomonas syringae		
Resin	**Winter**	**Winter**
0-25	<.0001	Sig Diff
0-50	<.0001	Sig Diff
0-100	<.0001	Sig Diff
25-50	<.0001	Sig Diff
25-100	<.0001	Sig Diff
50-100	<.0001	Sig Diff

Table A.8. *Pseudomonas syringae* least square means.

Winter Resin				
Resin Amount	**LSM**		**% Compared to Control**	**% Effect**
0	41.784	d	1.00	0.00
25	121.216	c	2.90	-1.90
50	214.475	b	5.13	-4.13
100	272.525	a	6.52	-5.52

Table A.9. Statistical results (SAS) comparing growth of *Bacillus cereus* treated with varying amounts of resin from different seasons.

Bacillus cereus				
Resin	**Summer Fresh**	**Summer Fresh**	**Winter Fresh**	**Winter Fresh**
0-25	<.0001	Sig Diff	<.0001	Sig Diff
0-50	<.0001	Sig Diff	<.0001	Sig Diff
0-100	<.0001	Sig Diff	<.0001	Sig Diff
25-50	0.8648	No Diff	0.5576	No Diff
25-100	0.8920	No Diff	<.0001	Sig Diff
50-100	0.9999	No Diff	<.0001	Sig Diff

Table A.10. *Bacillus cereus* least square means.

B. cer.	**Summer Resin**				**Winter Resin**			
Resin Amount	**LSM**		**% Compared to Control**	**% Effect**	**LSM**		**% Compared to Control**	**% Effect**
0	42.500	a	1.00	0.00	284.000	a	1.00	0.00
25	16.583	b	0.39	0.61	158.926	b	0.56	0.44
50	19.583	b	0.46	0.54	166.074	b	0.58	0.42
100	19.333	b	0.45	0.55	41.000	c	0.14	0.86

Table A.11. Statistical results (SAS) comparing growth of *E. coli* treated with varying amounts of resin from different seasons.

	E. coli					
Resin Amount	**Summer Fresh**		**Winter Fresh**		**Summer Stored**	
0-25	<.0001	Sig Diff	<.0001	Sig Diff	<.0001	Sig Diff
0-50	0.0001	Sig Diff	<.0001	Sig Diff	<.0001	Sig Diff
0-100	0.0001	Sig Diff	<.0001	Sig Diff	<.0001	Sig Diff
25-50	0.6473	No Diff	<.0001	Sig Diff	<.0001	Sig Diff
25-100	0.7072	No Diff	<.0001	Sig Diff	<.0001	Sig Diff
50-100	0.9997	No Diff	<.0001	Sig Diff	1.0000	No Diff

Table A.12. *Escherichia coli* least square means.

E. coli	**Summer Fresh**				**Winter Fresh**				**Summer Stored**			
Resin Amount	**LSM**		**% Compared to Control**	**% Effect**	**LSM**		**% Compared to Control**	**% Effect**	**LSM**		**% Compared to Control**	**% Effect**
0	364.750	a	1.00	0.00	252.315	a	1.00	0.00	263.821	a	1.00	0.00
25	339.917	b	0.93	0.07	187.802	b	0.74	0.26	185.636	b	0.70	0.30
50	344.875	b	0.95	0.05	128.043	c	0.51	0.49	100.167	c	0.38	0.62
100	344.458	b	0.94	0.06	81.8395	d	0.32	0.68	100.377	c	0.38	0.62

Table A.13. Statistical results (SAS) comparing growth of *Agrobacterium tumefaciens* treated with varying amounts of resin from different seasons.

	Agrobacterium tumefaciens			
Resin	**Summer Fresh**	**Summer Fresh**	**Winter Fresh**	**Winter Fresh**
0-25	0.0104	Sig Diff	<.0001	Sig Diff
0-50	0.0155	Sig Diff	0.0063	Sig Diff
0-100	0.5773	No Diff	0.8252	No Diff
25-50	0.9988	No Diff	0.3511	No Diff
25-100	0.2031	No Diff	0.0003	Sig Diff
50-100	0.2630	No Diff	0.0753	No Diff

Table A.14. *Agrobacterium tumefaciens* least square means.

A. tumen.	Summer Fresh				Winter Fresh			
Resin Amount	LSM		% Compared to Control	% Effect	LSM		% Compared to Control	% Effect
0	34.250	a	1.00	0.00	183.235	a	1.00	0.00
25	17.625	b	0.51	0.49	138.148	c	0.75	0.25
50	18.375	b	0.54	0.46	153.247	bc	0.84	0.16
100	27.750	ab	0.81	0.19	175.370	ab	0.96	0.04

Table A.15. Statistical results (SAS) comparing growth of *Erwinia amylovora* treated with varying amounts of resin from different seasons.

	Erwinia amylovora					
Resin amount	Summer Fresh		Winter Fresh		Summer Stored	
0-25	0.0015	Sig Diff	<.0001	Sig Diff	<.0001	Sig Diff
0-50	<.0001	Sig Diff	<.0001	Sig Diff	<.0001	Sig Diff
0-100	<.0001	Sig Diff	<.0001	Sig Diff	<.0001	Sig Diff
25-50	<.0001	Sig Diff	<.0001	Sig Diff	<.0001	Sig Diff
25-100	<.0001	Sig Diff	<.0001	Sig Diff	<.0001	Sig Diff
50-100	0.5637	No Diff	0.663	No Diff	0.3246	No Diff

Table A.16 *Erwinia amylovora* least square means.

E. amy	Summer Fresh				Winter Fresh				Summer Stored			
Resin Amount	LSM		% Compared to Control	% Effect	LSM		% Compared to Control	% Effect	LSM		% Compared to Control	% Effect
0	402.83	a	1.00	0.00	237.09	a	1.00	0.00	344.38	a	1.00	0.00
25	325.22	b	0.81	0.19	167.11	b	0.70	0.30	228.71	b	0.66	0.34
50	170.93	c	0.42	0.58	126.64	c	0.53	0.47	112.209	c	0.33	0.67
100	144.25	c	0.36	0.64	119.14	c	0.50	0.50	97.061	c	0.28	0.72

Table A.17. Statistical results (SAS) comparing growth of *Bacillus cereus* treated with varying amounts of *α*-pinene.

Growth of *B. cereus*	
α-pinene	
0 vs 25 µL	0.0094
0 vs 50 µL	<0.0001
25 vs 50 µL	0.0012

Table A.18. Least square means of *Bacillus cereus* treated with varying amounts of *α*-pinene.

Least Square Means Comparison

α-pinene Treatment	CFU/mL		% Compared to Control	% Effect
0 (control)	2311111	**a**	1.00	0.00
25 µL	1833333	**b**	0.79	0.21
50 µL	1233333	**c**	0.53	0.47

Table A.19. Statistical results (SAS) comparing growth of *Bacillus cereus* treated with varying amounts of *α*-pinene.

α-pinene Applied to *B. cereus*
Type 3 Tests of Fixed Effects

Effect	Num DF	Den DF	F Value	Pr > F	
Treatment	2	6	2031.37	< .0001	Sig Diff
Time in hours	23	138	1355.99	< .0001	Sig Diff
Treatment * Time in hours	46	138	119.46	< .0001	Sig Diff

Table A.20. Least square means of *Bacillus cereus* treated with varying amounts of *α*-pinene.

α-pinene at Full Strength

	4 Hrs				8 Hrs				12 Hrs			
Treatment	**LSM**		**% Compared to Control**	**% Effect**	**LSM**		**% Compared to Control**	**% Effect**	**LSM**		**% Compared to Control**	**% Effect**
0 (Control)	59.33	a	1.00	0.00	136.33	a	1.00	0.00	124.33	a	1.00	0.00
25 µL	42.00	b	0.71	0.29	86.67	b	0.64	0.36	135.50	b	1.09	-0.09
50 µL	20.67	c	0.35	0.65	37.50	c	0.28	0.72	69.67	c	0.56	0.44
	16 Hrs				**20 Hrs**				**24 Hrs**			
	LSM		**% Compared to Control**	**% Effect**	**LSM**		**% Compared to Control**	**% Effect**	**LSM**		**% Compared to Control**	**% Effect**
0 (Control)	131.00	a	1.00	0.00	192.00	a	1.00	0.00	215.00	a	1.00	0.00
25 µL	164.00	b	1.25	-0.25	186.83	a	0.97	0.03	206.00	a	0.96	0.04
50 µL	74.33	c	0.57	0.43	95.67	b	0.50	0.50	172.00	b	0.80	0.20

Table A.21. Statistical results (SAS) comparing growth of *Bacillus cereus* treated with varying amounts of β-pinene.

β-pinene Applied to *B. cereus*
Type 3 Tests of Fixed Effects

Effect	Num DF	Den DF	F Value	Pr > F	
Treatment	2	6	2.07	0.2078	No Diff
Time in hours	22	132	14.35	< .0001	Sig Diff
Treatment * Time in hours	44	132	3.26	< .0001	Sig Diff

Table A.22. Least square means of *Bacillus cereus* treated with varying amounts of β-pinene.

β-pinene at Full Strength

	4 Hrs				8 Hrs				12 Hrs			
Treatment	**LSM**		**% Compared to Control**	**% Effect**	**LSM**		**% Compared to Control**	**% Effect**	**LSM**		**% Compared to Control**	**% Effect**
0 (Control)	115.50	a	1.00	0.00	143.00	a	1.00	0.00	132.83	a	1.00	0.00
25 µL	89.67	a	0.78	0.22	54.17	b	0.38	0.62	36.17	b	0.27	0.73
50 µL	81.17	a	0.70	0.30	33.17	b	0.23	0.77	43.00	b	0.32	0.68
	16 Hrs				**20 Hrs**				**24 Hrs**			
	LSM		**% Compared to Control**	**% Effect**	**LSM**		**% Compared to Control**	**% Effect**	**LSM**		**% Compared to Control**	**% Effect**
0 (Control)	113.83	a	1.00	0.00	162.00	a	1.00	0.00	201.00	a	1.00	0.00
25 µL	99.67	a	0.88	0.12	164.17	a	1.01	-0.01	191.33	a	0.95	0.05
50 µL	106.00	a	0.93	0.07	157.17	a	0.97	0.03	169.83	a	0.84	0.16

APPENDIX 2

Protocol A.1. FTIR evaluation of resin collected for two years in summer (June/July) and winter (February/March). Since the *a priori* assumption in this research was that antimicrobial activity was different in summer and winter, chemistry of resin was collected in two season was determined. At the winter collection period, the tree was not actively growing, but it was in an active growth state during summer collections. Resin was not collected from the new growth because the amount of resin was less than in the older tissues.

In this study, resins collected from one tree over a two year period were evaluated. Needles from LN were collected during June/July (summer) and February/March (winter) over a two year period (2013-2014). Resin was expressed from needles by hand and placed onto the diamond sample window and scanned (650–4000 cm-1 spectral range, 8 cm-1 spectral resolution, 32 scans per spectrum) using a Thermo Nicolet Nexus Model 670 FTIR spectrometer equipped with a Golden Gate MKII Single Reflection ATR accessory. Spectra used for PCA included 5-10 independently expressed and scanned subsamples.

For both years, temperature and rainfall were greater in the summer than in the winter. The winter of 2014 was warmer than the winter of 2013 by almost 2°C, and had approximately 1.5 cm more precipitation. Summer temperatures were within 1 °C in the two years, but rainfall in 2013 was almost twice 2014. Principal component analysis was used to determine the effect of season and year on the chemical composition of the resins. There were no differences when resin collected in the same year (Figure A.3) or resins collected in the same season in different years (Figure A.4) were compared.

Protocol A.2. FTIR and Pyrolysis GCMS of lyophilized resins collected in 2014 [summer (June/July) and winter (February/March)]. Lyophilized resin was prepared from resins collected in the summer and winter as described in Chapter 2. Three analytical methods were used to characterize subsamples of the bulked LNS, LNW, VAS, and VAW resin samples: FTIR; pyrolysis GCMS (Pyro-GCMS); and GCMS. One set of subsamples was directly applied to sample well in a Thermo Nicolet model iS5 FTIR equipped with a Nicolet 1D7 Single Reflection ATR accessory. Samples were scanned at 650–4000 cm-1 spectral range, 8 cm-1 spectral resolution, at 16 scans per spectrum). Because samples were fluid, the ATR pressure anvil was not needed to ensure sufficient contact with the diamond window. Spectra used for PCA included those from 5-10 independently scanned subsamples. A second set of subsamples (300 μg) was weighed in stainless steel cups and pyrolyzed using a Frontier EGA/PY-3030 D pyrolyzer. Separations of the pyrolysis vapors were carried out on a Perkin Elmer Clarus 680 gas chromatograph with an Elite 17 MS capillary column (30 m 9 0.25 mm ID 9 0.25 μm film thickness). The split ratio was 80:1with helium as the carrier gas (1 mL/min). Oven temperature for the gas chromatograph was held at 50 °C for 4 min and then ramped to 280 °C (5 °C/min). Peaks representing individual pyrolysis degradation products were identified using a Perkin Elmer Clarus SQ 8 GC mass spectrometer. Principal component analysis (PCA) was performed on the spectral data to observe differences and groupings between the sample sets. Comparisons were made between sites/locations and seasons. A third set of subsample was analyzed using gas chromatography mass spectrometry (GCMS) as previously described (Yates, Chapter 2).

The LN and VA had similar environments during each collection period. Both trees were in full sun and mean monthly temperatures reported for the nearest cities were rarely more than 1

°C apart. Mean monthly rainfall for the winter months was more abundant for the VA. Rainfall was greater at VA in the summer.

GCMS. Results from the GCMS analysis are shown in Chapter 3.

FTIR. The instrument to collect FTIR spectra in this study was a small portable unit, and spectra were similar to those collected with the Model 670. Validation of the use of this instrument is important because spectra can be obtained at remote locations without the need to ship biological specimens, and composition can be preserved. Peaks and peak ratios were consistent with those in the longitudinal study and that of previous reports (Tappert et al., 2011). In PCA analyses of FTIR data, there were no differences between seasons in the same site (Figure A.5). There were differences based on several functional groups between sites in summer but not in winter (Figure A.6).

Pyrolysis GCMS. Based on separation by PCA of Pyro-GCMS spectral data, VA summer resin was different than LN summer (Figure A.7), but the winter resins were not different from one another (Figure A.8). Composition of VA resins collected in the summer were different from those collected in the winter (Figure A.9). Composition of LN resins collected in the summer were different than those collected in the winter (Figure A.10).

VITA

David Yates has been a nurseryman for over thirty years, owning Laurels Nursery in East Tennessee. Later in life, he went back to school to earn a Bachelor's of Science Degree in biology at East Tennessee State University, in Johnson City, TN. Next, he earned a Master's of Science in biology and a Maste's of Arts in Teaching Science (Secondary) Degrees, also from East Tennessee State University.

David next began a teaching career at David Crockett High School, in Jonesborough, Tennessee, where he was named Teacher of the Year his second year teaching. He teaches Advanced Biology I, Biology II, A.P. Biology, Hillbilly Heritage, and serves as the Science Department Chair.

David earned his Doctor of Philosophy Degree in Plants, Soils, and Insects from the University of Tennessee, Knoxville in 2016. David studied and conducted his research in the Entomology and Plant Pathology Department's Bioactive Natural Products Lab under the direction of Dr. Kimberly D. Gwinn. His research involves studying the biochemistry and bioactive activity of the resin of a rare Japanese tree, *Sciadopitys verticillata.*

David plans on continuing his research at the University of Tennessee, further researching *Sciadopitys* and other plants with potential bioactivity. David continues teaching high school at David Crockett High School, a job, a place, and students he really loves.